NAVAL POSTGRADUATE SCHOOL

MONTEREY, CALIFORNIA

THESIS

**PERFORMANCE EVALUATION OF A PROTOTYPE
UNDERWATER SHORT-RANGE
ACOUSTIC TELEMETRY MODEM**

by

Pongsakorn Sommai

September 2010

Thesis Co-Advisors:	Steven R. Baker
	Joseph A. Rice

Approved for public release; distribution is unlimited

THIS PAGE INTENTIONALLY LEFT BLANK

REPORT DOCUMENTATION PAGE		*Form Approved OMB No. 0704-0188*
Public reporting burden for this collection of information is estimated to average 1 hour per response, including the time for reviewing instruction, searching existing data sources, gathering and maintaining the data needed, and completing and reviewing the collection of information. Send comments regarding this burden estimate or any other aspect of this collection of information, including suggestions for reducing this burden, to Washington headquarters Services, Directorate for Information Operations and Reports, 1215 Jefferson Davis Highway, Suite 1204, Arlington, VA 22202-4302, and to the Office of Management and Budget, Paperwork Reduction Project (0704-0188) Washington DC 20503.		
1. AGENCY USE ONLY *(Leave blank)*	**2. REPORT DATE** September 2010	**3. REPORT TYPE AND DATES COVERED** Master's Thesis
4. TITLE AND SUBTITLE Performance Evaluation of a Prototype Underwater Short-Range Acoustic Telemetry Modem		**5. FUNDING NUMBERS**
6. AUTHOR(S) Pongsakorn Sommai		
7. PERFORMING ORGANIZATION NAME(S) AND ADDRESS(ES) Naval Postgraduate School Monterey, CA 93943-5000		**8. PERFORMING ORGANIZATION REPORT NUMBER**
9. SPONSORING /MONITORING AGENCY NAME(S) AND ADDRESS(ES) N/A		**10. SPONSORING/MONITORING AGENCY REPORT NUMBER**
11. SUPPLEMENTARY NOTES The views expressed in this thesis are those of the author and do not reflect the official policy or position of the Department of Defense or the U.S. Government. IRB Protocol number _____N.A._____.		
12a. DISTRIBUTION / AVAILABILITY STATEMENT Approved for public release; distribution is unlimited		**12b. DISTRIBUTION CODE** A

13. ABSTRACT (maximum 200 words)

This thesis documents the evaluation of the transmitter performance of a short-range underwater acoustic modem. This prototype modem was fabricated by contractor Teledyne Benthos, Inc. and is identified as Model ATM-90X. It was developed for use in the Seastar underwater Local Area Network (LAN). The ATM-90X modem is required to be capable of transferring large amounts of digital data at a range up to 500 m using the 33–55 kHz acoustic frequency band. The modem's transmitter performance was evaluated in term of its transmit frequency response, vertical beam pattern, and maximum source level. Underwater acoustic measurements were conducted in an anechoic water tank and the data were analyzed using signal processing techniques including Hilbert transforms, autocorrelation, and cross correlation. The transmission characteristics of the intended underwater acoustic communication channel were modeled to determine the required modem operating performance in the best and worst case situations. The measured performance characteristics were evaluated in the context of the communication link margin (i.e., the excess signal-to-noise ratio) associated with the modeled channels. The results show that (1) the modem transmit frequency response does not have acceptable flatness across the entire 33–55 kHz band; (2) the beam pattern in the vertical plane has a good hemisphere pattern; (3) estimated maximum source level is 175 dB re 1μPa-m at broadside of the modem. Based on the evaluated performance, the ATM-90X modem can provide a successful communication link with the highest data rate at the range of 500 m in the best-case situation (least noise). However, in the worst-case situation, the communication link will fail to reach performance objectives.

14. SUBJECT TERMS Acoustic Communications, Acoustic Modem, Seastar LAN			**15. NUMBER OF PAGES** 110
			16. PRICE CODE
17. SECURITY CLASSIFICATION OF REPORT Unclassified	**18. SECURITY CLASSIFICATION OF THIS PAGE** Unclassified	**19. SECURITY CLASSIFICATION OF ABSTRACT** Unclassified	**20. LIMITATION OF ABSTRACT** UU

THIS PAGE INTENTIONALLY LEFT BLANK

PERFORMANCE EVALUATION OF A PROTOTYPE UNDERWATER SHORT-RANGE ACOUSTIC TELEMETRY MODEM

Pongsakorn Sommai
Lieutenant Junior Grade, Royal Thai Navy
B.S., University of Michigan, 2005
M.A., Chulalongkorn University, 2009

Submitted in partial fulfillment of the
requirements for the degree of

MASTER OF SCIENCE IN ENGINEERING ACOUSTICS

from the

NAVAL POSTGRADUATE SCHOOL
September 2010

Author: Pongsakorn Sommai

Approved by: Steven R. Baker
                 Thesis Co-Advisor

                 Joseph A. Rice
                 Thesis Co-Advisor

                 Daphne Kapolka
                 Chair, Engineering Acoustics Academic Committee

iii

THIS PAGE INTENTIONALLY LEFT BLANK

ABSTRACT

This thesis documents the evaluation of the transmitter performance of a short-range underwater acoustic modem. This prototype modem was fabricated by contractor Teledyne Benthos Inc. and is identified as Model ATM-90X. It was developed for use in the Seastar underwater Local Area Network (LAN). The ATM-90X modem is required to be capable of transferring large amounts of digital data at a range up to 500 m using the 33–55 kHz acoustic frequency band. The modem's transmitter performance was evaluated in terms of its transmit frequency response, vertical beam pattern, and maximum source level. Underwater acoustic measurements were conducted in an anechoic water tank and the data were analyzed using signal processing techniques including Hilbert transforms, autocorrelation, and cross correlation. The transmission characteristics of the intended underwater acoustic communication channel were modeled to determine the required modem operating performance in the best- and worst-case situations. The measured performance characteristics were evaluated in the context of the communication link margin (i.e., the excess signal-to-noise ratio) associated with the modeled channels. The results show that (1) the modem transmit frequency response does not have acceptable flatness across the entire 33–55 kHz band; (2) the beam pattern in the vertical plane has a good hemisphere pattern; (3) estimated maximum source level is 175 dB re 1μPa-m broadside to the modem. Based on the evaluated performance, the ATM-90X modem can provide a successful communication link with the highest data rate at the range of 500 m in the best-case situation (least noise). However, in the worst-case situation, the communication link will fail to reach performance objectives.

THIS PAGE INTENTIONALLY LEFT BLANK

TABLE OF CONTENTS

LIST OF FIGURES

THIS PAGE INTENTIONALLY LEFT BLANK

LIST OF TABLES

THIS PAGE INTENTIONALLY LEFT BLANK

LIST OF ACRONYMS AND ABBREVIATIONS

B&K	Brüel & Kjær
bps	Bits per Second
FDM	Frequency-Division Multiplexing
H_3BO_3	Boric Acid
LAN	Local Area Network
LM	Link Margin
MFSK	M-ary Frequency-Shift Keying
$MgSO_4$	Magnesium Sulfate
NL	Noise Level
NSL	Noise Spectrum Level
ONR	Office of Naval Research
ppm	Parts Per Million
rms	Root Mean Square
SER	Symbol Error Rate
SNR	Signal-to-Noise Power Ratio
SNR_s	SNR per Symbol
$SNRL_s$	SNR per Symbol in dB
SL	Source Level
SPL	Sound Pressure Level
$SPL_{rcv,\ 1\ symbol}$	Sound Pressure Level for Receiving 1 Symbol
SSP	Sound Speed Profile
TG	Transmission Gain
TL	Transmission Loss
$TL_{absorption}$	Transmission Loss due to Absorption
$TL_{cylindrical}$	Transmission Loss due to Cylindrical Spreading
$TL_{spherical}$	Transmission Loss due to Spherical Spreading
UUV	Unmanned Underwater Vehicle
WAN	Wide Area Network

THIS PAGE INTENTIONALLY LEFT BLANK

ACKNOWLEDGMENTS

I.   INTRODUCTION

A.   BACKGROUND

The Teledyne Benthos ATM-90X underwater acoustic telemetry modem, shown in Figure 1, is a prototype device developed under the sponsorship of the Office of Naval Research (ONR) for use as a communication node in a Seastar underwater acoustic local area network (Seastar LAN).

Figure 1.   Teledyne Benthos ATM-90X underwater acoustic telemetry modem

Seastar LAN (Figure 2) is an underwater communication network characterized by short range links (50–500 meters) and high frequency acoustic signaling (33–55 kHz) [1]. There is one central node and multiple peripheral nodes in the centralized Seastar architecture. Data from a set of peripheral nodes are transmitted to the central node for processing and fusion. The central node is able to exfiltrate processed information through a Seaweb wide area network (Seaweb WAN) [2], [3]. Thus, the Seastar LAN is essentially a sub-network of Seaweb WAN. Seastar LAN is intended to be deployed in shallow water environments with water depths typically less than 200 m. Potential applications for Seastar LAN include supporting communications between networks of He3 magnetic sensors, acoustic sensors, unmanned underwater vehicles (UUV), and divers. Seastar is required to have the capability of transferring large amounts of digital data from the peripheral nodes to the central node.
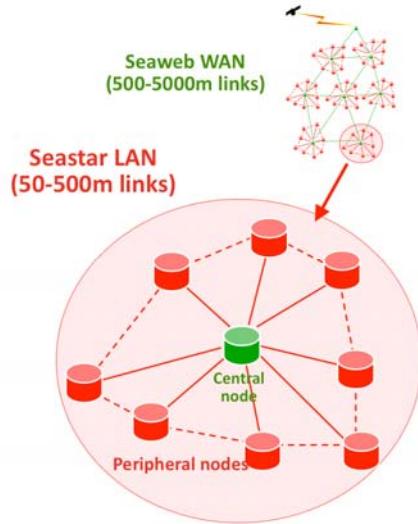
Figure 2.   Seastar LAN and Seaweb WAN concept. From [4]

The ATM-90X modem is designed to meet Seastar LAN operational requirements. Teledyne Benthos, the manufacturer, measured the performance of the wide band transducer selected for the ATM-90X modem in 2009 [5]. However, the transmitter performance of the ATM-90X modem has never been evaluated in the context of the Seastar operational requirement.

B.   SCOPE OF THESIS

The scope of this thesis is to evaluate the transmitter performance of the ATM-90X modem, as well as to establish procedures for analyzing short-range acoustic telemetry modems developed in the future.

The performance of the ATM-90X modem transmitter was characterized by its transmit frequency response, vertical beam pattern, and source level, as measured in a small anechoic underwater acoustic tank, in the Acoustic Laboratories of the Naval Postgraduate School. This thesis also examines the underwater acoustic communication channel in order to estimate the best and worst operational conditions under which the ATM-90X modem is expected to be deployed. A comparison between measured and

required performances provides the communication link margin which indicates the expected performance of the ATM-90X modem in the operational environment.

C.   STRUCTURE OF THESIS

To understand the nature of a short-range underwater acoustic telemetry modem requires knowledge of transducers, underwater acoustics, digital communication, and signal processing. This thesis contains seven chapters including this introduction.

Chapter II discusses topics related to an underwater acoustic communications channel.   The underwater communication channel is presented and modeled.   The expected best and worst case channel conditions are described.

Chapter III presents the underwater acoustic communications concept for Seastar. Digital communication, the modulation scheme used in the ATM-90X modem, and performance metrics are explained. Required transmitter characteristics of the ATM-90X modem for best and worst case channel conditions are derived.

Chapter IV provides an overview of the ATM-90X acoustic telemetry modem, including its specifications and functions.

Chapter V describes the procedures employed for performance evaluation of the ATM-90X modem. Setups for measurements are illustrated. Measurement techniques are explained. Measured performances are presented.

Chapter VI compares the measured performances against the required performances in the best and worst case operating environments. It demonstrates how the ATM-90X modem is expected to perform under these conditions.

Chapter VII summarizes the findings and makes recommendations for future work.

THIS PAGE INTENTIONALLY LEFT BLANK

II.   UNDERWATER ACOUSTIC COMMUNICATION CHANNEL

The effectiveness of underwater acoustic communications depends greatly on the condition of the ocean environment. In order to successfully establish an acoustic communication link under given environmental conditions, the physical communication channel must be taken into consideration. The two most important characteristics of utilizing the ocean as the communication channel are the transmission loss (including multipath interference effects) and ambient noise level. In this chapter, we will explain the characteristics of the underwater acoustic communication channel and model an underwater acoustic communication channel under which the ATM-90X modem is expected to be deployed. The expected best and worst case channel conditions will also be described.

The underwater communication channel is analogous to a waveguide that is bounded by the sea surface and the sea floor (Figure 3). There are several factors that impair signal reception in the ocean. Variations in sound speed results in refraction of sound, which can weaken signal strength. The air-sea interface and the sea bottom boundary cause reflections, which generate multipath propagation that further distorts and disperses the signal. Various noise sources in the ocean also deteriorate reception capability.
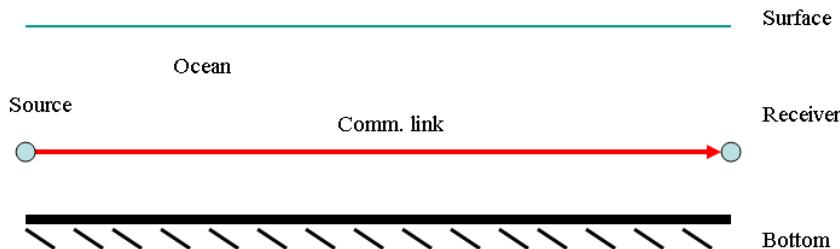
Figure 3.   Ocean as a cylindrical waveguide

We categorize these factors into two major terms; transmission loss and noise. With analysis of these two terms, we come up with estimated loss in a modeled communication channel, which is used in further analysis.

A. TRANSMISSION LOSS

The phenomenon that acoustic intensity decreases as it propagates though the medium is quantified by a parameter called transmission loss (*TL*). *TL* is the loss in intensity level or sound pressure level between two field points, generally referred to as the source and receiver. *TL* is usually expressed in terms of the logarithmic ratio of the sound intensity at a reference range of one meter away from the center of the acoustic source (I_0) and the sound intensity at the receiver (I_1) [6]. *TL* values are expressed in decibels.

$$TL = 10\log\left(\frac{I_0}{I_1}\right) \text{ dB} \tag{2.1}$$

For ocean environments of interest for Seastar, there are three types of losses contributing to the total *TL*. These losses are categorized as spreading loss, absorption loss (including scattering), and multipath loss.

1. Spreading Loss

Spreading loss is the *TL* due to the geometric spreading of acoustic energy as sound travels away from the source. Typically, the spreading loss depends only on range of propagation. Therefore, it is frequency independent. The two simplest models for spreading loss are spherical and cylindrical.

a. Spherical Spreading

Spherical spreading occurs when an acoustic wave radiates spherically outward from the source in an unbounded medium. The formula for spherical transmission loss is given by:

$$TL_{spherical} = 20\log r \text{ dB} \tag{2.2}$$

where *r* is the range from the source in m.

b. Cylindrical Spreading

In the bounded medium that has the characteristic of a waveguide such as the ocean, which is bounded by the ocean surface and floor, acoustic waves travel outward between two parallel surfaces. Therefore, at ranges much greater than the depth, the energy propagates cylindrically. The formula for cylindrical transmission loss is given in (2.3):

$$TL_{cylindrical} = 10 \log r \quad \text{dB} \tag{2.3}$$

where r is the range from the source in m.

2. Absorption Loss

The absorption loss is the *TL* due to viscous, thermal, and chemical relaxations. It is frequency dependent. The formula for transmission loss due to absorption is:

$$TL_{absorption} = a(r-1) \quad \text{dB} \tag{2.4}$$

where a is the absorption coefficient in dB/m and r is the range from the source in m. Other loss mechanisms such as scattering and bottom interactions can be included in the absorption coefficient but are treated separately in this thesis.

There are many theoretical and empirical formulas to quantify the absorption coefficient a. For our purpose, we use the approximation introduced in [7], which approximates the absorption coefficient for sound in seawater with pH = 8, salinity S = 35 ppm, and temperature = 5 C for frequencies below 100 kHz. The absorption coefficient has three components: the first two are chemical relaxations for boric acid (H_3BO_3) and magnesium sulfate ($MgSO_4$), respectively, and the third is the contribution of pure water. The formula is:

$$a = f^2 \left(\frac{0.08}{0.9 + f^2} + \frac{30}{3000 + f^2} e^{-\frac{z}{6}} + 4 \times 10^{-4} \right) \quad \text{dB/km} \tag{2.5}$$

where f is the frequency in kHz and z is the depth in km.

We investigate the effect of absorption loss at different frequencies. We choose three representative frequencies (33 kHz, 43 kHz and 53 kHz) for detailed study. Plots of absorption loss and geometric spreading loss are presented in Figure 4.

7
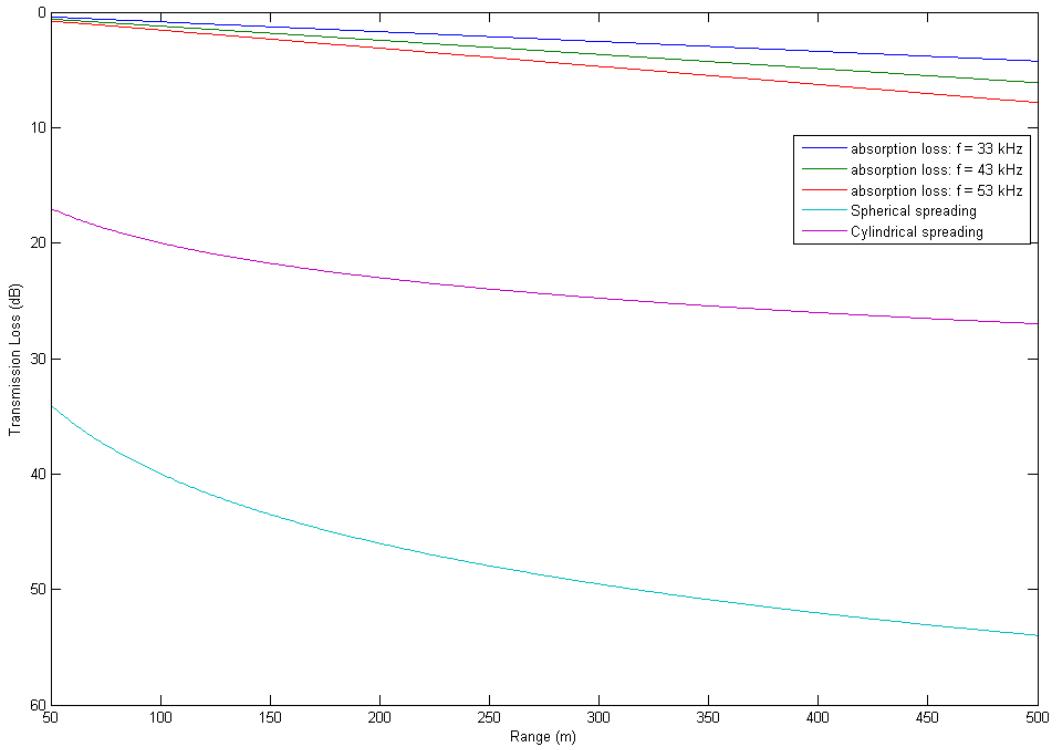
Figure 4.   Comparison of absorption loss, cylindrical spreading loss, and spherical spreading loss at the frequencies of 33 kHz, 43 kHz and 53 kHz, at a ranges between 50–500 m

Absorption loss increases with frequency (Figure 4). At a range of 500 m, $TL_{absorption}$ for frequencies of 33 kHz, 43 kHz, and 55 kHz is about 4 dB, 6 dB, and 8 dB, respectively. Spherical spreading and cylindrical spreading are frequency independent. $TL_{spherical}$ is 34 dB at $r = 50$ m from the source and increases to 54 dB at $r = 500$ m. $TL_{cylindrical}$ is 17 dB at $r = 50$ m from the source and 27 dB at $r = 500$ m.

When absorption loss is included for both types of geometric spreading, the TL at $r = 500$ m increases by 4 to 8 dB, depending on frequency. The comparison is shown in Figure 5.
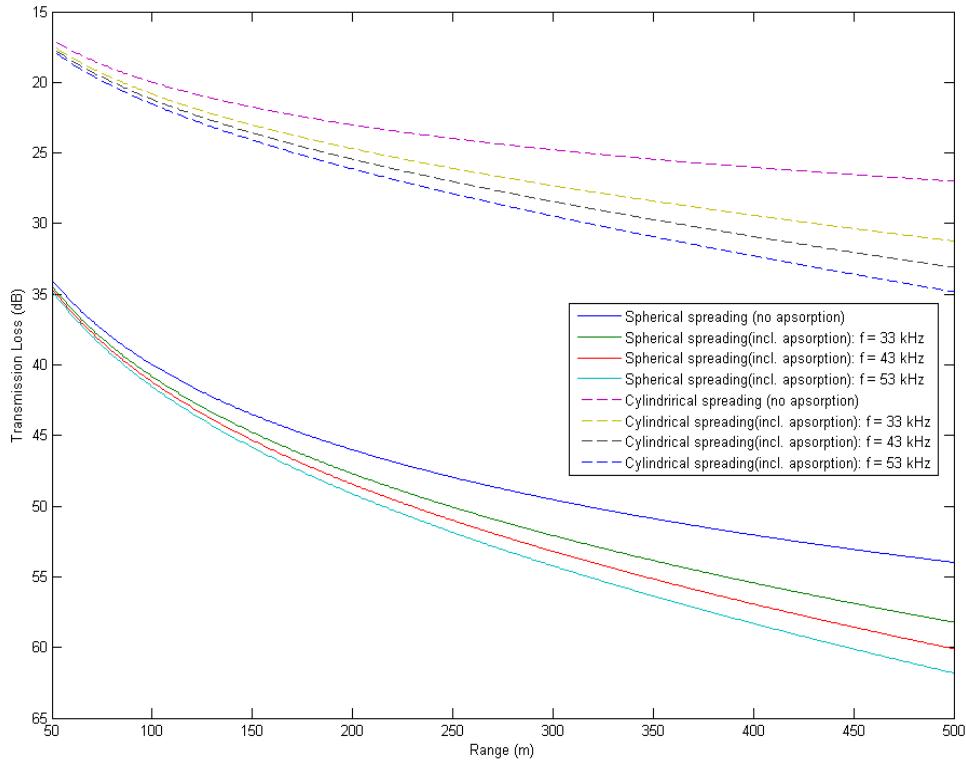
Figure 5.   Comparison of cylindrical spreading with absorption loss and spherical spreading with absorption loss at the frequencies of 33 kHz, 43 kHz and 53 kHz with a range between 50–500 m

3.   Multipath Loss

Multipath sound propagation (reception) refers to situations in which there are additional sound transmission pathways in addition to direct path propagation.

In deep water and over long ranges, multipath reception by a receiver generally results from refractive propagation paths, as opposed to paths that include boundary reflections. In this case, cumulative boundary reflection losses, especially with the ocean bottom, effectively eliminate boundary multipath propagation from contributing to distant received acoustic signal. Multipath propagation due to boundary reflections suffers

severe *TL* as bounce losses for long range propagation in the deep ocean accumulate. Therefore, the most important multipath contributors to distant received signals are only from refractive rays.

In case of shallow water, however, refraction is generally insignificant, and so multipath propagation almost certainly involves boundary reflection. With limited depths, interactions between acoustic rays and the boundaries are more typical than refractive rays. In shallow water, multipath propagation due to boundary reflection, and the resultant interference with direct path propagation, is a major contributor to the received acoustic signal.

In shallow water, at typical ranges of interest, multipath propagation from source to receiver is an important sound transmission pathway because, other than direct path propagation, there might only be one or two boundary reflected paths that contribute to a received signal. Therefore, the effect of these interactions must be considered and the boundaries of both surface and floor must be treated as potentially lossy reflectors. When an acoustic ray interacts with one of the boundaries, its signal characteristics, such as frequency, phase, and amplitude may change. Each ray travels with a unique path, as illustrated by Figure 6. Each ray arriving at the receiver is called an eigenray. Since each eigenray has a unique path, it also has a unique arrival time.

There is the possibility of constructive and destructive interferences due to different phases of rays arriving at the receiver at different arrival times. These interferences might cause severe fluctuation in transmission loss.
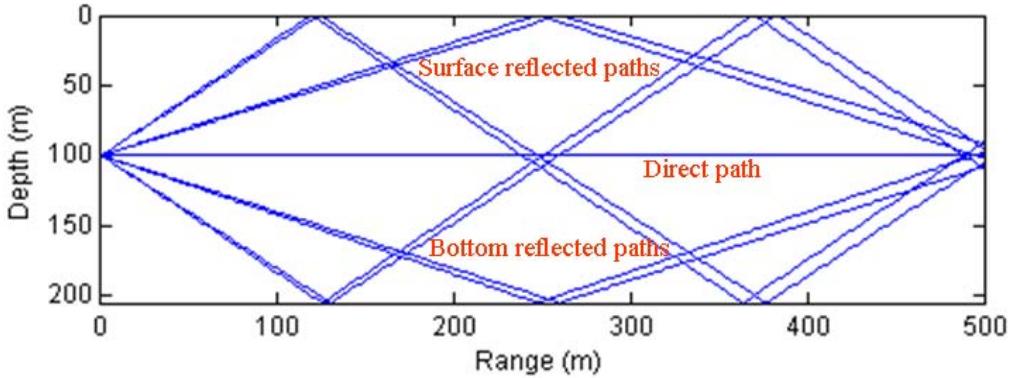
Figure 6.   Multipath propagation of eigenrays at a range of 500 m plotted by
Bellhop ray trace. From [4]

We can model the underwater acoustic communication channel as a transmitted signal $x(t)$, a received signal $y(t)$, and the impulse response $h(t)$, as shown in Figure 7. From basic communication theory for a linear channel, the received signal $y(t)$ is the convolution of $x(t)$ with $h(t)$ [8].

$$x(t) \longrightarrow \boxed{h(t)} \longrightarrow y(t) = h(t) * x(t)$$
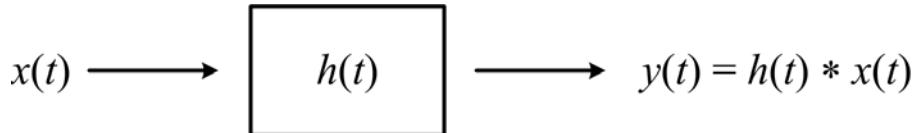
Figure 7.   Simple model of a linear, time- and space-invariant communication
channel. The received signal $y(t)$ is a convolution of the transmitted
signal $x(t)$ with the channel impulse response $h(t)$. From [4]

Hence, $h(t)$ is the acoustic channel response. In other words, $h(t)$ presents the characteristics of propagation in the channel.

4.   Bellhop Transmission Loss Model

The Bellhop underwater acoustic propagation model was developed in 1987 by Porter and Bucker at the Space and Naval Warfare System Center in San Diego. The Bellhop model uses Gaussian beam ray tracing to produce the ray-trace, impulse response, and *TL* for a source-receiver configuration in an ocean waveguide. It is a

11

range-independent program, which means that it assumes that the sound-speed profile (SSP), the surface and bottom properties, and the bathymetry of the ocean floor do not vary with range. The Bellhop underwater acoustic propagation modeling software has a MATLAB graphical user interface (GUI). It is available from the Centre for Marine Science and Technology at the Curtin University of Technology at Perth, Australia [9].

Torres [10] used and concluded in his work that the Bellhop model is accurate and suitable to model high-frequency acoustic propagation in shallow water. "It has proven to be an accurate modeling tool for high-frequency (>1 kHz) transmissions" [10]. Some others, such as Kerstens [3], Thompson [11] and Jenkins [4], also used the Bellhop model in their research. Since the Bellhop model is a proven model used for previous works related to communication in shallow water, we use the Bellhop model as our reference for estimating the *TL*.

The parameters we used for channel environments in our Bellhop model are the same as those used in Jenkins' acoustic channel analysis [4]. The parameters for the modeled environment are shown in Table 1.

Table 1. Environmental parameters for modeling and simulation of the underwater acoustic communications channel. From [4]

Parameter	Value
Depth	205 m
Range	50 – 500 m
Bottom Type	Quartz sand
Compressional Sound Speed (Water)	1500 m/s
Compressional Sound Speed (Bottom)	1730 m/s
Density (Water)	1026 kg/m^3
Density (Bottom)	2070 kg/m^3
Surface RMS Roughness	0 m
Bottom RMS Roughness	0 m
Shear Sound Speed	0 m/s
Compressional Absorption	0 dB/m
Shear Absorption	0 dB/m

We will provide comparisons between the *TL* obtained from the Bellhop model and the *TL* due to spherical spreading with absorption loss and due to cylindrical spreading with absorption loss.

We consider the sensitivity of the *TL* to various parameters, including 3 source-receiver depths, 3 frequencies, and 2 ocean surface roughness conditions, respectively. For each of these three cases, we also compare incoherent with coherent *TL*. Incoherent *TL* is computed by summing only the intensity of all rays, while coherent *TL* takes both magnitude and phase of rays into account for the calculation.

The first parametric study shows the effect of source-receiver depth. We use the Bellhop model to generate both incoherent and coherent *TL* at a frequency of 43 kHz with no surface roughness. The source-receiver depths are 5 m (near surface), 100 m (center of the channel), and 200 m (near bottom). In each case, propagation is simulated with launch angles between +85° and -85° using 15,000 rays.

The results are shown in Figure 8. Due to limitations of MATLAB, what is actually plotted is the transmission gain (*TG*), *TG = -TL*. For each depth, incoherent *TG* is shown on the left, coherent *TG* on the right. Also plotted are the *TG* for spherical spreading plus absorption (bottom smooth curve), cylindrical spreading plus absorption (top smooth curve), and the *TG* that would result from the superposition of two sound path contributors of equal strength (spherical spreading plus absorption, +3dB for incoherent, + 6 dB for coherent).

The results show the great variability in coherent *TG* with range. The variability at a range close to 500 m is approximately 20 dB. Secondly, it is clearly that cylindrical spreading plus absorption does not at all approximate the *TG*.

At the greater ranges, the coherent *TG* pattern suggests that the received signal is predominated by the interference between the direct path arrival and one almost equal strength multipath arrival, as evidenced by the close agreement between the peak value of the Bellhop-computed *TG* and the *TG* curve representing spherical spreading plus absorption plus 6 dB. The incoherent *TG* at greater ranges also suggests the predominant nature of the received signal is the interference between the direct path arrival and one

13

multipath arrival of essentially equal strength (as evidenced by the close agreement between the Bellhop-computed *TG* and the *TG* curve representing spherical spreading plus absorption plus 3 dB.

We observe some dependence of *TG* with source-receiver depth at shorter ranges, but not at longer ranges. At short range, the proximity of the nearest reflecting surface determines the relative contribution of the multipath arrival compared to direct path. Note, for 5 m and 200 m depths, peak values in coherent *TG* also agree well with the *TG* curve for spherical spreading plus absorption plus 6 dB, where as, for 100 m depth, the *TG* fluctuates only slightly about the *TG* curve for spherical spreading plus absorption alone, with no multipath contribution. The incoherent *TG* curves show the same feature, that is, variability with source-receiver depth only at short ranges.
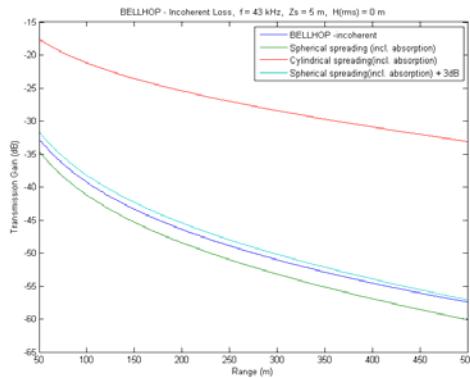
(a) incoherent, 5 m depth.　　　　　　　(b) coherent, 5 m depth.
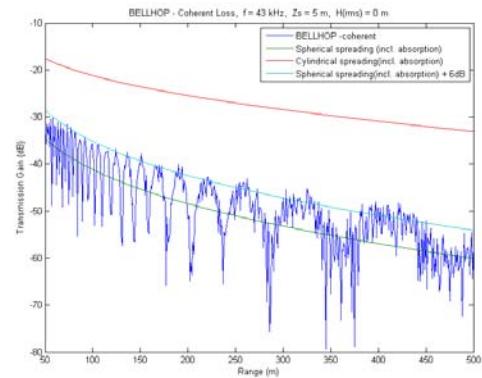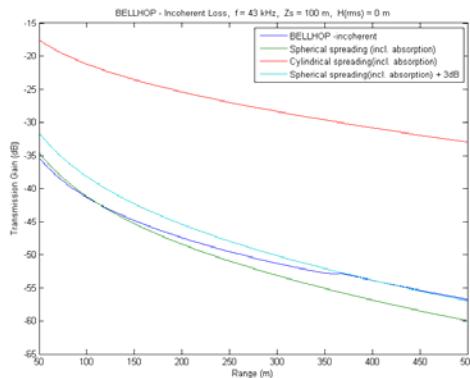
(c) incoherent, 100 m depth.　　　　　(d) coherent, 100 m depth.
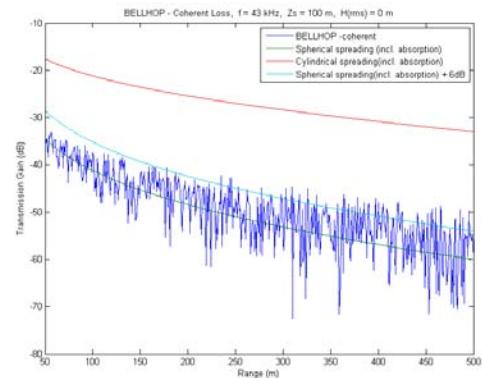
(e) incoherent, 200 m depth.   (f) coherent, 200 m depth.
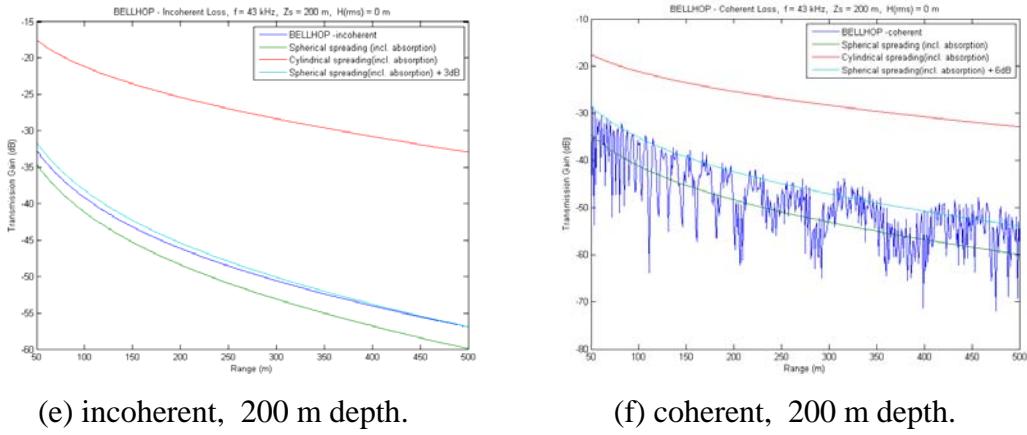
Figure 8.   Comparison of incoherent and coherent *TL* estimated by Bellhop model, and *TL* from spherical spreading with absorption loss, and *TL* from cylindrical spreading with absorption loss, at a frequency of 43 kHz with source-receiver depths of 5 m, 100 m and 200 m

In the second parametric study, we examine the dependence on frequency. We consider three different frequencies: 33 kHz, 43 kHz, and 53 kHz. The source-receiver depth is at 100 m (center of the channel). At $r = 500$ m, the frequency range between 33 kHz to 53 kHz does not produce significant effect on *TG* (Figure 9).

For the last parametric study, we investigate the effect of surface roughness. We use the Bellhop model to simulate *TG* at f = 43 kHz and the source-receiver depth of 100 m. We use a roughness of 0 m (no roughness) and 5 m (approximately 15 m/s wind speed). The results (Figure 10) surprisingly show that roughness has no apparent effect on *TG* at $r = 500$ m.
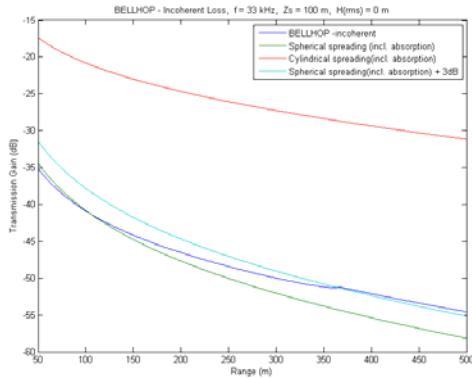
(a) incoherent, frequency: 33 kHz.
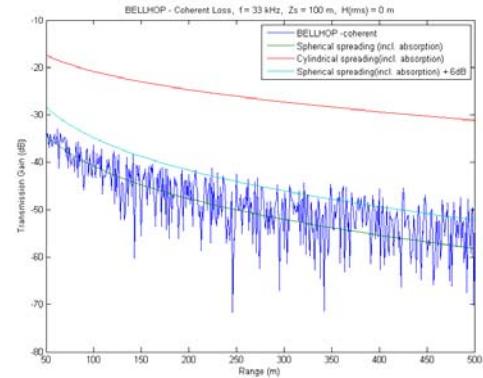
(b) coherent, frequency: 33 kHz.
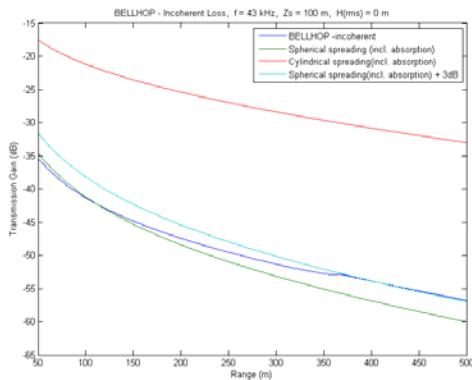
(c) incoherent, frequency: 43 kHz.
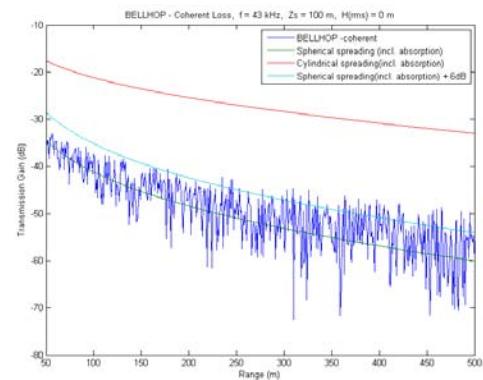
(d) coherent, frequency: 43 kHz.
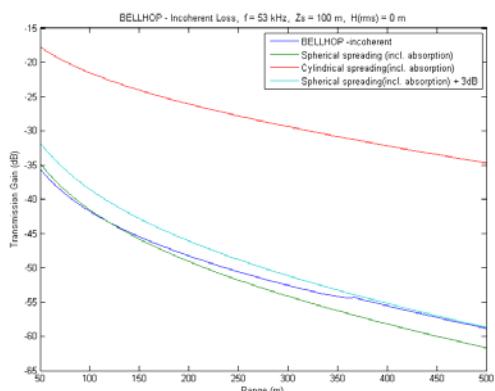
(e) incoherent, frequency: 53 kHz.
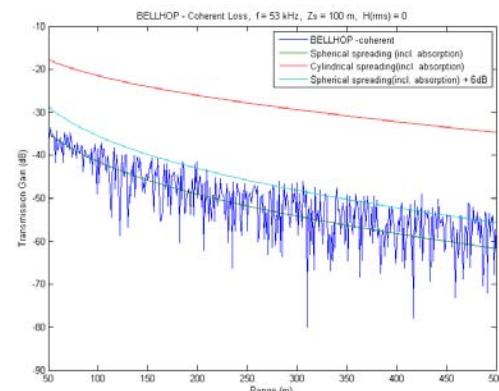
(f) coherent, frequency: 53 kHz.

Figure 9.   Comparison of incoherent and coherent *TL* estimated by Bellhop model, and *TL* from spherical spreading with absorption loss, and *TL* from cylindrical spreading with absorption loss, at a source-receiver depth of 100 m at frequencies of 33 kHz, 43 kHz, and 53 kHz
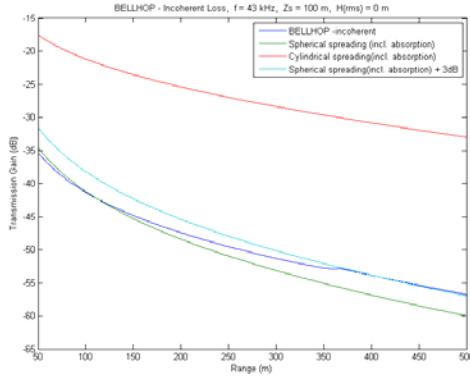
(a) incoherent, no surface roughness.   (b) coherent, no surface roughness.
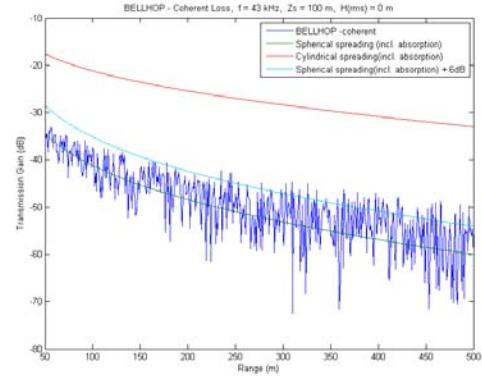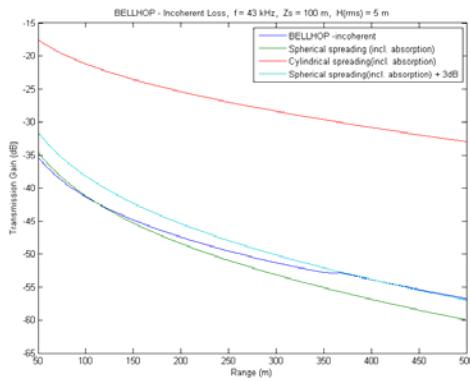
(a) incoherent, with surface roughness.   (b) coherent, with surface roughness.
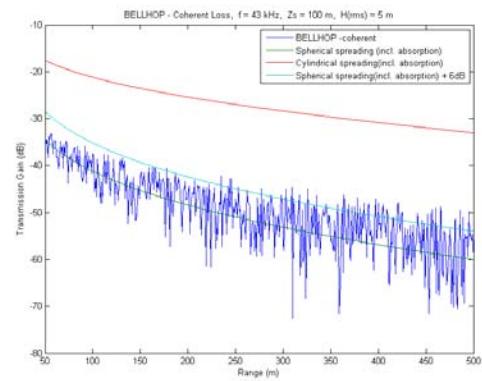
Figure 10.   Comparison of incoherent and coherent *TL* estimated by Bellhop model, and *TL* from spherical spreading with absorption loss, and *TL* from cylindrical spreading with absorption loss, at a source-receiver depth of 100 m at frequency of 43 kHz, at roughness of 0 m and 5 m in surface height

5.   Approximate Transmission Loss Estimation

In the shallow water channel, the received signal is the result of the interference between the direct path and multipath propagations (Figure 6) that arrive at the receiver within the same symbol transmission time duration. Since the Seastar modem uses an envelope detection scheme for the receiver, the relevant measure of the received signal is its magnitude. The magnitude of the received signal $\left| y(t) \right|$ is given by:

$$\left| y(t) \right| = \left| p_{direct}(t) + \sum_{multipath} p_{multi,i}(t) \right| \tag{2.6}$$

where $p_{direct}(t)$ is the direct path received pressure signal and $p_{multi,i}(t)$ is the received pressure signal via multipath i.

In practice, for real operating environment, there are fluctuations in the height and slope of the ocean surface, and in the depth of the moored modem, due to surface wave and current action. These fluctuations introduce uncertainty in the estimated *TL*. However, the time-scale and length-scale of environmental fluctuations are much longer than a single-symbol transmission duration (6.25 ms for the 20 kHz-bandwidth) and signal wavelength (about 3 cm at 30 kHz), respectively. Therefore, the result is a quasi-stationary interference among different received signal contributions on a time scale of a single-symbol transmission duration, but a random relative phase among the received signal contributors on time scales on the order of approximately one second or greater. Therefore, our best estimation of *TL(TG)* when fluctuations are taken into account is to use the "*expected value*" of the detected received signal for calculation.

Assuming random phase of contributors, the expected value of the detected received signal (i.e. magnitude) $E(\left| y(t) \right|)$ is the incoherent sum of the received signal contributors, given by

$$E(\left| y(t) \right|) = \sqrt{\left| p_{direct} \right|^2 + \sum_i \left| p_{multi,i} \right|^2} \tag{2.7}$$

This corresponds to the incoherent *TL* calculated by Bellhop. Based on the results of Bellhop *TL* (Figure 8-10), at the range of 500 m, we find that the incoherent *TL* is well approximated as that for spherical spreading with absorption losses minus 3 dB. Therefore, we determine that our best estimation for expected *TL* at the range of 500 m is that for spherical spreading with absorption minus 3 dB, which is

$$TL = 20 \log r + a(r-1) - 3 \text{ dB} \tag{2.8}$$

TL by spherical spreading with absorption loss minus 3 dB is shown for ranges from 50 to 500 m and frequencies from 30 to 60 kHz in Figure 11. Figure 12 shows the

TL at 500 m for the same frequency range. The *TL* at $r = 500$ m increases from about 54.5 dB at 30 kHz to about 59.5 dB at 60 kHz.
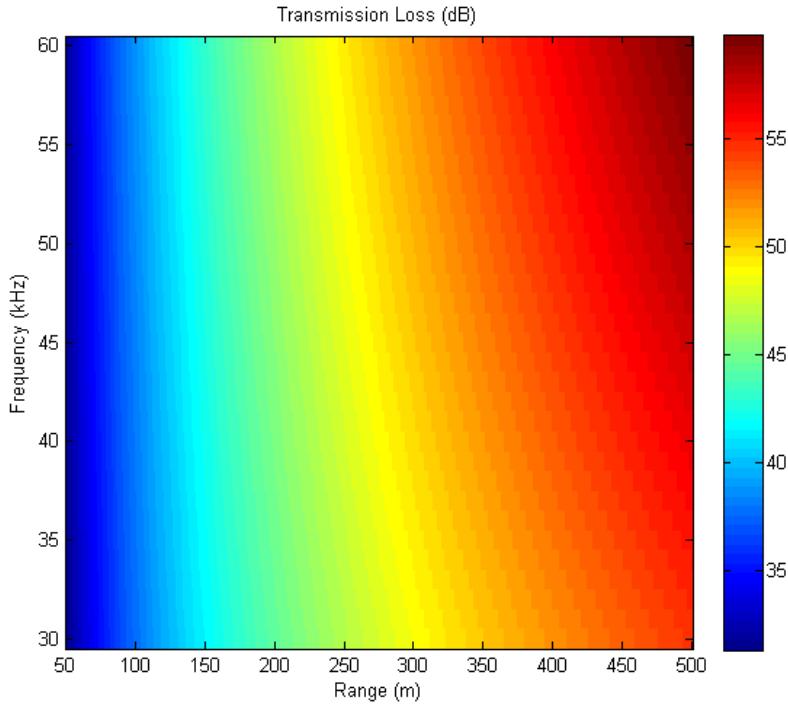
Figure 11.   Spherical spreading with absorption loss minus 3 dB for the frequencies of 30–60 kHz at the ranges between 50–500 m
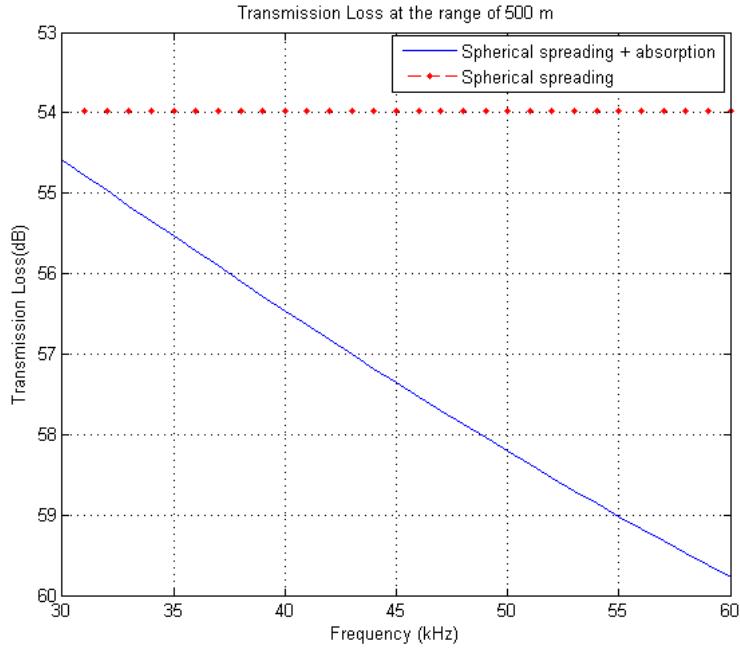
Figure 12.   Spherical spreading with absorption loss minus 3 dB for frequencies of 30–60 kHz at the range of 500 m

In conclusion, spherical spreading with absorption loss minus 3 dB is used for channel *TL* estimation. The estimated *TL* is range and frequency dependent. At *r* = 500 m, *TL* is estimated to be approximately 49.5 dB at 60 kHz, and about 54.5 dB at 30 kHz.

B.   NOISE

Ambient noise in the underwater communications channel originates from both natural and man-made sources. Naturally occurring noise is caused by biological and seismic activities and by hydrodynamic noise from waves, currents, tides, rain and wind [1]. Man-made noise is due mainly to shipping activities.

Contributions of each noise source can be described empirically. Figure 16 shows the estimated Noise Spectrum Level (*NSL*) in deep water based on formulae provided by Coates [12]. The *NSL* is generally dependent on four sources, each dominating certain frequency bands, namely turbulence (<10 Hz), shipping (10–200 Hz), wind (0.2–100 kHz) and thermal activity (>100 kHz) [3]. Of course, these sources are variable

depending on weather and other factors, but Figure 13 also indicates that, for our frequency of interest, between 35 and 55 kHz, wind-related noise contributes the most to the *NSL*.
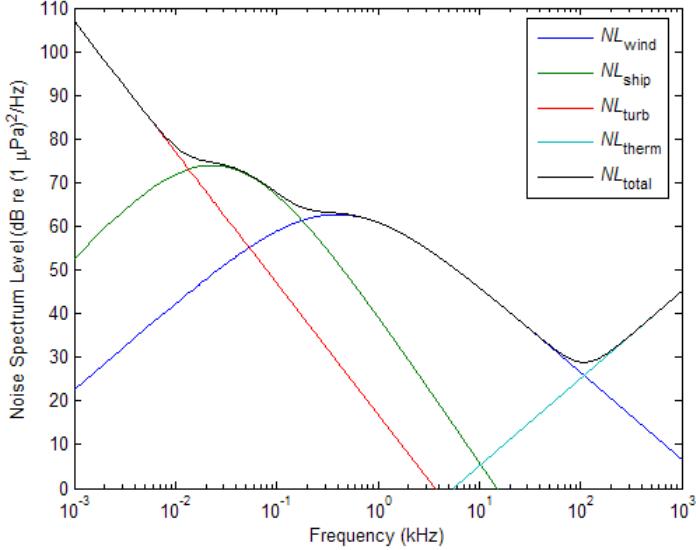
Figure 13.   The noise spectrum level (*NSL*) in dB based on empirical formulas by Coates. From [3]

However, Coates' empirical formulae are based on data taken in deep water and do not include biological noise such as from snapping shrimp, whose noise signature is of high amplitude and broadband, and which can be found in many shallow-water environments [4]. Therefore, we can only partially use Coates' formulae for estimation of noise in the shallow water in which Seastar will operate.

In shallow water, noise is not as well defined as it is in deep water. This is because there is greater variability in both time and place in shallow water environments than in deep water. However, Urick states there are three major categories of noise in shallow water: wind noise, biological noise and shipping noise [13]. The combination of these three noise sources determines noise levels in shallow water.

Therefore, for the purpose of noise estimation, we categorize sources of noise using Urick's categories. It is difficult to establish a general noise estimate for shallow

water because of the high variability between different areas. Therefore, we estimate best and worst noise case conditions based on available data for wind noise, biological noise and shipping noise.

1.   Wind Noise

We apply Coates' formulae for our estimation of wind noise. According to the empirical formulae from [12], illustrated in Figure 14, wind noise depends on frequency and wind speed. In the frequency range of 35–55 kHz, for wind speeds between 0 and 15 m/s (about 0 to 30 knots), the *NSL* ranges from about 20 to 49 dB re 1 $\mu Pa^2/Hz$. So, the estimated *NSL* is 20 dB re 1 $\mu Pa^2/Hz$ for the best case condition where there is no wind and the sea state is 0 or 1. And for the worst case operational condition, where the wind speed is 15 m/s and the sea state is 7, the *NSL* is estimated to be about 49 dB re 1 $\mu Pa^2/Hz$.
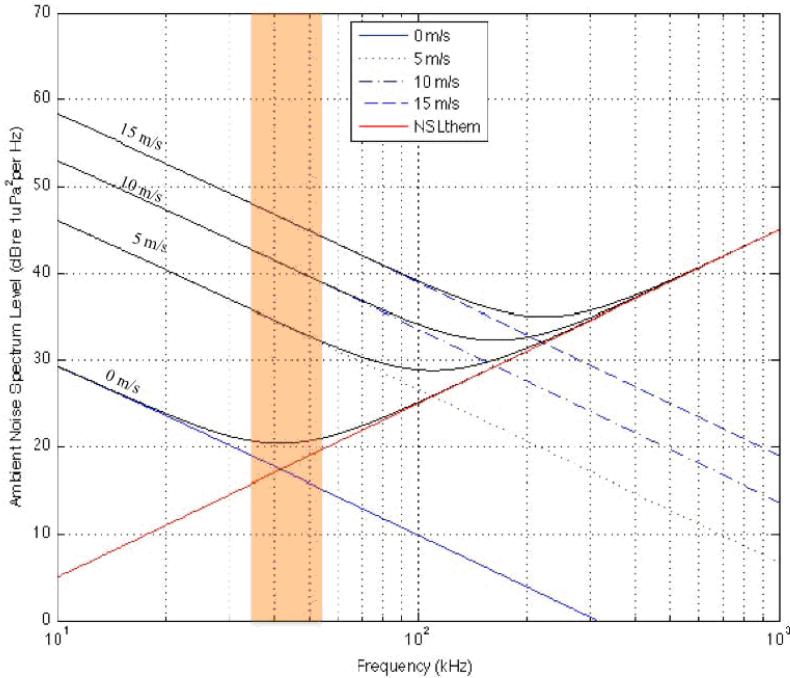
Figure 14.   Noise Spectrum Level caused by wind. From [1]

2.   Biological Noise

Snapping shrimp, which exist in waters below latitudes of 27 degrees, generate a high level of noise in the frequency band of our interest. From Figure 15, we see that snapping shrimp can generate $NSLs$ between 48 and 80 dB re $1\mu Pa^2/Hz$ in the frequency band of about 35–55 kHz [1].
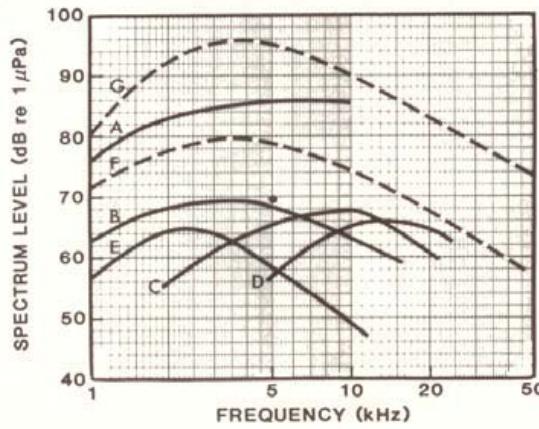
Figure 15.   Snapping shrimp NSL measured at various locations. From [1]

3.   Shipping Noise

Most of the shipping noise energy in the deep ocean is below 1 kHz. Contribution of shipping noise to our frequency band of interest is mostly found in areas close to harbors or ports. Goh investigated the NSL of shipping noise from five ports in the United States and Panama [1]. He found that, in the frequency band of 35–55 kHz, the maximum NSL is 77 dB re 1 $\mu Pa^2/Hz$ and the minimum NSL is 44 dB re 1 $\mu Pa^2/Hz$.

4.   Estimation of Noise Spectrum Level

Therefore, the total NSL is the summation of the three major sources of noise: wind, biological and shipping noises [1].

$$NSL_{min} = Wind_{min} \oplus Shipping_{min} \oplus Bio_{min} \tag{2.9}$$

23

$$NSL_{min} = 20 \text{ dB} \oplus 44 \text{ dB} \oplus 0 \text{ db} = 44 \text{ dB re } 1 \text{ } \mu\text{Pa}^2/\text{Hz} \qquad (2.10)$$

$$NSL_{max} = Wind_{max} \oplus Shipping_{max} \oplus Bio_{max} \qquad (2.11)$$

$$NSL_{max} = 49 \text{ dB} \oplus 77 \text{ dB} \oplus 80 \text{ db} = 82 \text{ dB re } 1 \text{ } \mu\text{Pa}^2/\text{Hz} \qquad (2.12)$$

The minimum *NSL* in the best (quietest) noise condition is 44 dB re 1 μPa^2/Hz. And the maximum *NSL* in the worst (noisiest) noise condition is 82 dB re 1 μPa^2/Hz.

III.   UNDERWATER ACOUSTIC PHYSICAL COMMUNICATION

The constraints imposed by the ocean environment directly affect the performance of underwater communication. In order to overcome the constraints of the ocean environment and achieve a required performance, digital communication techniques, such as a modulation scheme, must be implemented. In this chapter, we will describe the characteristics of the physical communication layer proposed for the Seastar LAN. Relationships between spectral bandwidth and performance in terms of the error rate and data rate are explained. We will estimate the best and worst operating conditions that Seastar LAN is expected to encounter. Lastly, required performances of the ATM-90X modem for best and worst case channel conditions are derived. We will limit all explanation to a specific case of Seastar LAN only.

A.   PHYSICAL COMMUNICATION LAYER

In this section, we explain digital communication techniques implemented in the communication layer of Seastar LAN. The concepts of multi-channel M-ary frequency shift keying modulation (multi-channel MFSK), spectral bandwidth, data rate, and the symbol error rate (SER) are introduced and discussed.

1.   Multi-Channel M-ary Frequency Shift Keying Modulation

Seastar modems are projected to use the same modulation scheme as the one used in Seaweb modems. The modulation is commonly referred to as multi-channel MFSK. We explain the concept of MFSK before presenting multi-channel MFSK.

MFSK [14] has proven to be a robust modulation scheme for underwater communications under various conditions [15], [16]. In MFSK, multiple frequency bands are used to transmit one of a possible M symbols [17]. The number of possible symbols is given by $M = 2^{n_b}$, where n_b is total number of data bits contained in a transmitted symbol. In Seastar, the number of possible symbols M is 4. Therefore, there

are 2 bits per symbol. This configuration is referred to as 4-ary FSK or 1-in-4 FSK, because only one of a possible four symbols is actively transmitting at any instant [17].

Multi-channel MFSK is a hybridization of MFSK and frequency-division multiplexing (FDM). In multi-channel MFSK, several channel MFSK pulse trains are transmitted simultaneously. In other words, multiple symbols, instead of one, are simultaneously transmitting at any instant, using a FDM technique [4]. Multi-channel MFSK allows us to transmit I channels of MFSK pulse trains simultaneously. The scheme thus permits data to be transmitted in parallel, allowing for data rates that are higher than a single MFSK pulse train by a factor of I [4]. In Seastar, $I = 32$. Hence, 32 channels of 4-ary FSK are transmitted simultaneously. Figure 16 shows a frequency-time diagram illustrating the multi-channel MFSK transmission scheme employed in Seastar.

Therefore, in Seastar, a group of four adjacent frequency bands (4-ary FSK) is used to encode a "symbol." Each group of 4 frequency bands is said to constitute a 4-ary FSK "channel." In Seastar, 32 parallel channels are used to simultaneously transmit 32 symbols in one "time slice." Thus, there are possible $32 \times 4 = 128$ adjacent frequency bands (Figure 16). The frequency spacing and transmission time duration depend upon the overall bandwidth selected. For 20 kHz overall bandwidth, the frequency spacing (Δf_{4-ary}) is 160 Hz and the symbol time duration (Δt_{symbol}) is 6.25 ms. For 10 kHz overall bandwidth, the frequency spacing (Δf_{4-ary}) is 80 Hz and the symbol time duration (Δt_{symbol}) is 12.5 ms. By this scheme, the transmitted acoustic energy per symbol is independent of overall operational bandwidth.
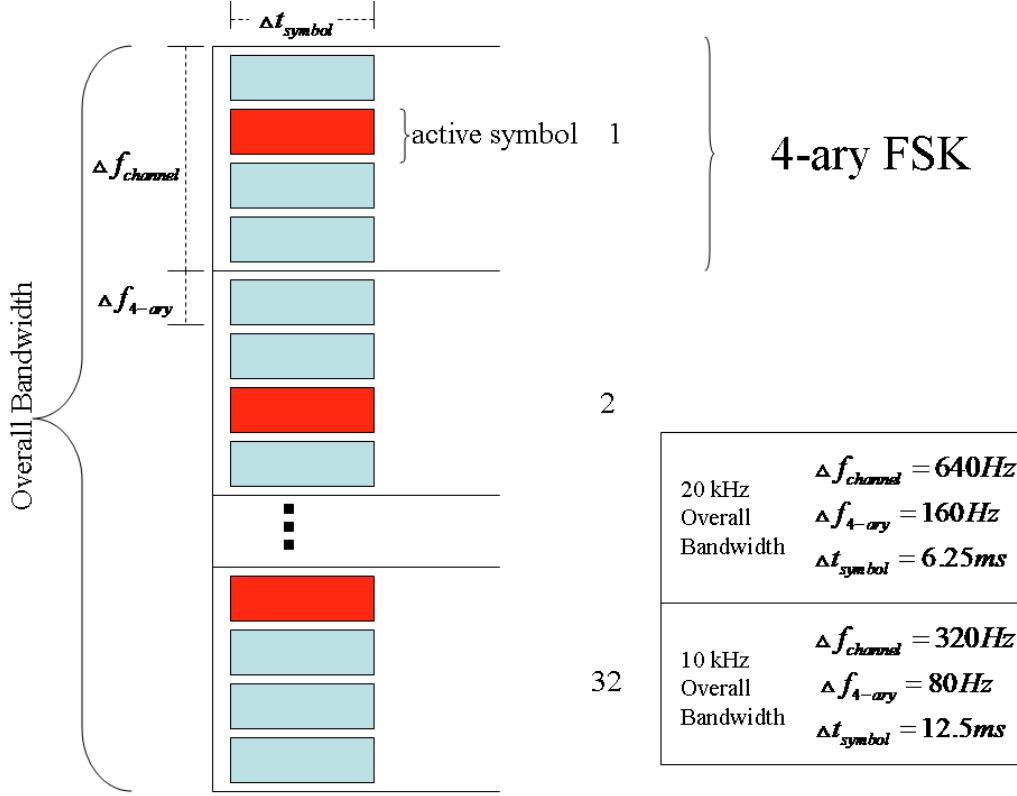
Figure 16.   Frequency-time diagram of transmission of 32-channel, 4-ary FSK

In the encoding scheme employed, a symbol is transmitted over a particular communication channel by transmitting a tone burst for one symbol duration time at exactly one of the four channel frequencies. Thus, four distinct symbols may be encoded. By choosing the symbol time duration (Δt_{symbol}) to equal $\dfrac{1}{\Delta f_{4-ary}}$, symbols are orthogonal (i.e., their "overlap time integral" is zero).   Therefore, an active symbol could be optimally coherently distinguished form the other three possible symbols using a matched filter.   However, this requires very high fidelity, non dispersive, predominantly direct-path propagation to be reliable.   In practice, envelope (incoherent) detection is conventionally employed in applications such as underwater acoustic communication, and is employed by the Teledyne Benthos ATM-90X modem.

The chosen encoding scheme is obviously very inefficient with respect to the use of the available encoding "space" (using 4 frequency bands to encode only 4 symbols),

27

but it has the advantage of robustness, that is, reduced probability of incorrect symbol communication (contaminated by noise and multipath interference).

Figure 17 shows a spectrogram of the 32-channel 4-ary FSK signal used in Seastar modems. The signal has a pulse duration of 6.25 ms, and a spectral bandwidth of $W = 20480$ Hz.
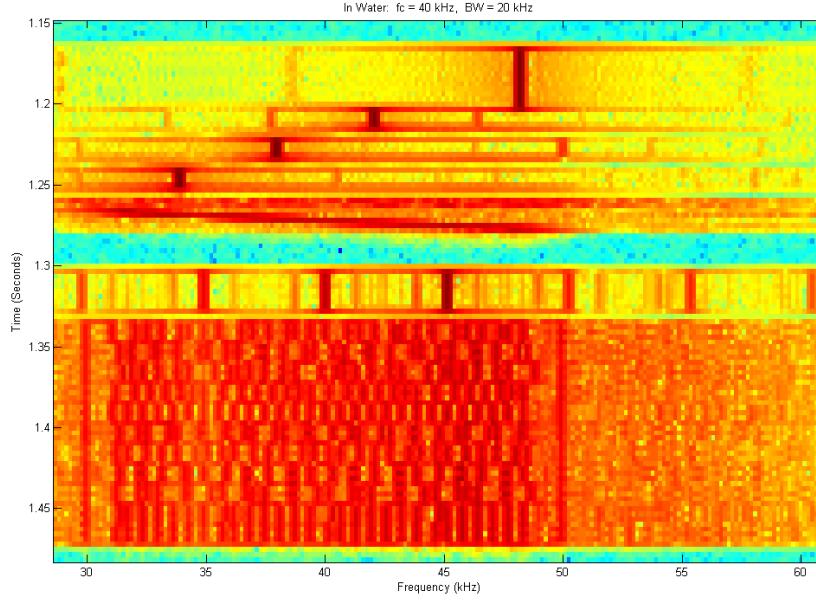
Figure 17.   Spectrogram of the multi-channel MFSK signal used Seastar modems.
The abscissa is frequency in kHz, and the ordinate is time in seconds

2.   Effect of the Bandwidth on Data Rate

In this section, we demonstrate the effect of different bandwidths on the transmit data rate.

In Seaweb (the WAN) modems, overall operational spectral bandwidth is 5120 Hz, with transmission in the 9–14 kHz band. The maximum uncoded (raw) data rate is 2400 bits per second (bps). The maximum data rate of 2400 bps is attributable to the multi-channel FSK modulation scheme. In the frequency domain, there are 32 channels of 4-ary FSK pulse trains. However, the two "outer" channels (the lowest and highest frequency channels) are used for Doppler tracking [18]. Thus, there are 30 channels

28

available to carry data at any one transmission. Since a 4-ary FSK pulse train contains 2 bits of data, 30 such channels contain 60 bits of uncoded data. The "time slice" duration is equal to the symbol time duration (Δt_{symbol}). In the case of Seaweb modems, $\Delta t_{symbol} = 25$ ms. Then, the number of parallel symbol transmissions per second is $1/\Delta t_{symbol}$, which is:

$$\frac{1}{25 \times 10^{-3}} = 40 \quad \text{transmissions per second} \tag{3.1}$$

Therefore, the maximum data that can be transmitted by Seaweb modems is $40(\sec^{-1}) \times 60(bits) = 2400$ bits per second (bps).

For the 20 kHz overall operational spectral bandwidth, the duration of transmission for Seastar modems is $\Delta t_{symbol} = 6.25$ ms. Then, the number of parallel symbol transmissions per second is:

$$\frac{1}{6.25 \times 10^{-3}} = 160 \text{ transmissions per second} \tag{3.2}$$

Therefore, the maximum data that can be transmitted by Seastar modems is $160(\sec^{-1}) \times 60(bits) = 9600$ bps.

In conclusion, increases or decreases in bandwidth result in a linear effect on maximum transmit data rate. If bandwidth is doubled, maximum data rate is also doubled. If bandwidth is quadrupled, maximum data rate is also quadrupled.

3.   Symbol Error Probability

For *M*-ary FSK, 1 out of a possible *M* symbols is active at any instant of transmission. Since Seastar modems use a noncoherent detection scheme, in order to successfully receive a given symbol, a detector must correctly determine which one out of the four frequency bands in a symbol channel is active. The probability to make a correct detection is called "probability of a correct decision (P_c)." The formula for P_c is [14]:

$$P_c = \sum_{n=0}^{M-1} (-1)^n \binom{M-1}{n} \frac{1}{n+1} e^{\left(\frac{-np_s}{n+1}\right)} \tag{3.3}$$

where $p_s = \dfrac{E_s}{N_0}$ is the signal-to-noise power ratio (SNR) per symbol (*SNR$_s$*). Here

$E_s = \displaystyle\int\limits_0^T p^2(t,W)dt$ is the total received signal "energy" in the (one) active channel

frequency subband, and N_0 is the single-sided (only positive frequency), average power spectral density of noise in that band in Watts/Hz [14].

That the SNR per symbol is given by $\dfrac{E_s}{N_0}$ requires some further explanation. The

noise energy accumulated in a single detector with bandwidth *W* over symbol time duration Δt_{symbol} is $N_0 W \Delta t_{symbol}$. So, the symbol energy is $SNR_s = E_s / N_0 W \Delta t_{symbol}$. This equals E_s / N_0 if $W \Delta t_{symbol} = 1$, which is the case for the Seastar modem (*W* = 640 Hz, Δt_{symbol} = 6.25 ms).

In dBs, SNR level per symbol (*SNRL$_s$*) is expressed logarithmically as:

$$SNRL_s = 10\log_{10}(\frac{E_s}{N_0}) \ \text{dB} \tag{3.4}$$

The probability of a symbol error is given by [14]:

$$P_M = 1 - P_c \tag{3.5}$$

$$P_M = \sum_{n=1}^{M-1}(-1)^{n+1}\binom{M-1}{n}\frac{1}{n+1}e^{(\frac{-np_s}{n+1})} \tag{3.6}$$

Figure 18 shows the symbol error probability (SER) as a function of SNR per symbol for *M* = 4.
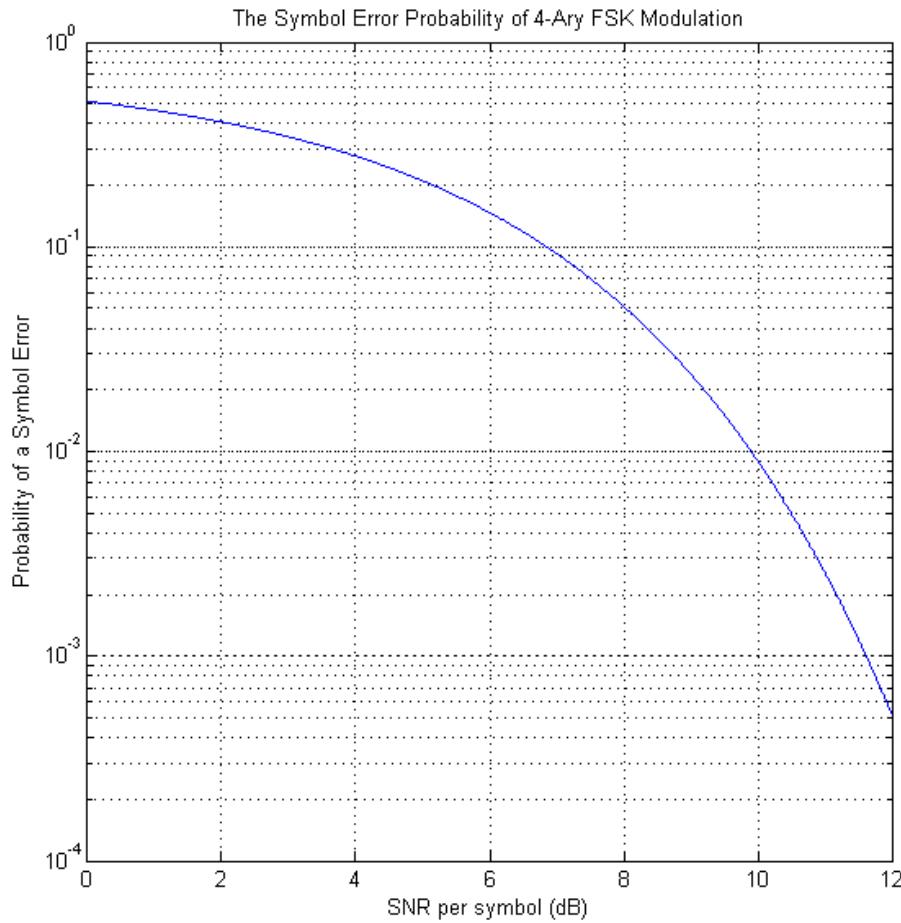
Figure 18.   Probability of symbol errors for noncoherent detection of 4-ary FSK
modulation. After [14]

B.   TELESONAR SHORT-RANGE ACOUSTIC LINK BUDGET

Acoustic link budget analysis is the method of analyzing performance of the acoustic communication system in term of excess SNR or link margin (*LM*). In this section, we perform a link budget analysis and derive the minimum required acoustic source level for maximum data rate of transmission at the range of 500 m in two environment conditions; the best (quietest) and the worst (noisiest) operating conditions.

Procedures to obtain required modem acoustic source level are as follows. First, we chose a "symbol" error rate (SER), which determines the required SNR per symbol

($SNRL_s$) at a receiver. The required $SNRL_s$ equals the required acoustic receiver SNR which, then, determines the required modem acoustic source level.

1. Symbol Error Probability and Required SNR per Symbol

For our further analysis in Chapter *VI*, we select three values of $SNRL_s$ which correspond to probabilities of a symbol error P_M of 0.10, 0.05 and 0.01. In other words, they are $SNRL_s$ required to ensure symbol-transmission success rates of 90%, 95% and 99%. The required $SNRL_s$ at a receiver, which correspond to these P_M, can be obtained through the error probability of 4-ary FSK modulation (Figure 18). These $SNRL_s$ values are found to be 6.86 dB, 8.04 dB, and 9.91 dB.

Table 2 shows values of $SNRL_s$ with their responding P_M of 0.1, 0.05, and 0.01.

Table 2. $SNRL_s$ at symbol- transmission success rates of 90%, 95% and 99%

P_M	$SNRL_s$ (dB)
0.10	6.86
0.05	8.04
0.01	9.91

2. Required Minimum Sound Pressure Level at Receiver for 1 Symbol

The receive SNR in a frequency band carrying an active symbol transmission is related to the received sound pressure by:

$$SNR_s = \frac{E_s}{N_0} = \frac{(p^2)_{avg,1symbol} \Delta t_{symbol}}{NSL} \qquad (3.7)$$

where

E_s is the signal energy in the 1 of *M* symbol detectors.

$N_0 = NSL$ is the noise spectrum level, i.e., the power spectral density of the noise, in Pa^2/Hz.

$(p)^2_{avg, 1 symbol}$ is the received mean-square pressure of a symbol.

Δt_{symbol} is the signal-symbol transmission time duration.

32

In terms of dBs, this relation is:

$$SNRL_s(dB) = SPL(dB \ re \ 1\mu Pa) + 10\log(\Delta t_{symbol})(dB \ re \ 1s) - NSL(dB \ re \ (1\mu Pa)^2 / Hz) \quad (3.8)$$

When the values of the $SNRL_s$ from Table 2 are substituted, this relationship give the required receive SPL for a specified symbol transmission success rate ($SPL_{rcv, \ 1 \ symbol}$).

3.   Required Narrowband Source Level for 1 Symbol

The required narrowband source level for transmitting 1 symbol ($SL_{req, \ 1sym}$) is a required single-frequency SL to transmit 1 symbol with the prescribed error rate. $SL_{req, \ 1sym}$ is given by:

$$SL_{req,1symbol} = SPL_{rcv,1symbol} + TL \quad dB \ re \ 1\mu Pa\text{-}m \quad\quad (3.9)$$

Therefore, for the Seastar modem, $SL_{req, \ 1sym}$ is:

$$SL_{req,1symbol} = SNRL_s + NSL + TL - 10\log(\Delta t_{symbol}) \quad dB \ re \ 1\mu Pa\text{-}m \quad\quad (3.10)$$

Maximum and minimum NSL are obtained from (2.10) and (2.12), which are 82 dB re 1 μPa^2/Hz and 44 dB re 1 μPa^2/Hz, respectively. These values correspond to the worst (noisiest) and best (quietest) operating conditions expected for Seastar LAN. TL is estimated as spherical spreading loss with absorption loss minus 3 dB at 500 m (Figure 12). It is range and frequency dependent. The $\Delta t_{symbol} = 12.5$ ms for a bandwidth of 10 kHz and $\Delta t_{symbol} = 6.25$ ms for a bandwidth of 20 kHz. Figure 19 shows $SL_{req, \ 1sym}$ for a bandwidth of 10 kHz with symbol-transmission probability of success rates of 90%, 95% and 99%, under the estimated best and worst case operating conditions for Seastar modems. Figure 20 shows $SL_{req, \ 1sym}$ for a bandwidth of 20 kHz with symbol-transmission probability of success rates of 90%, 95% and 99%, under estimated best and worst case operating conditions for Seastar modem.
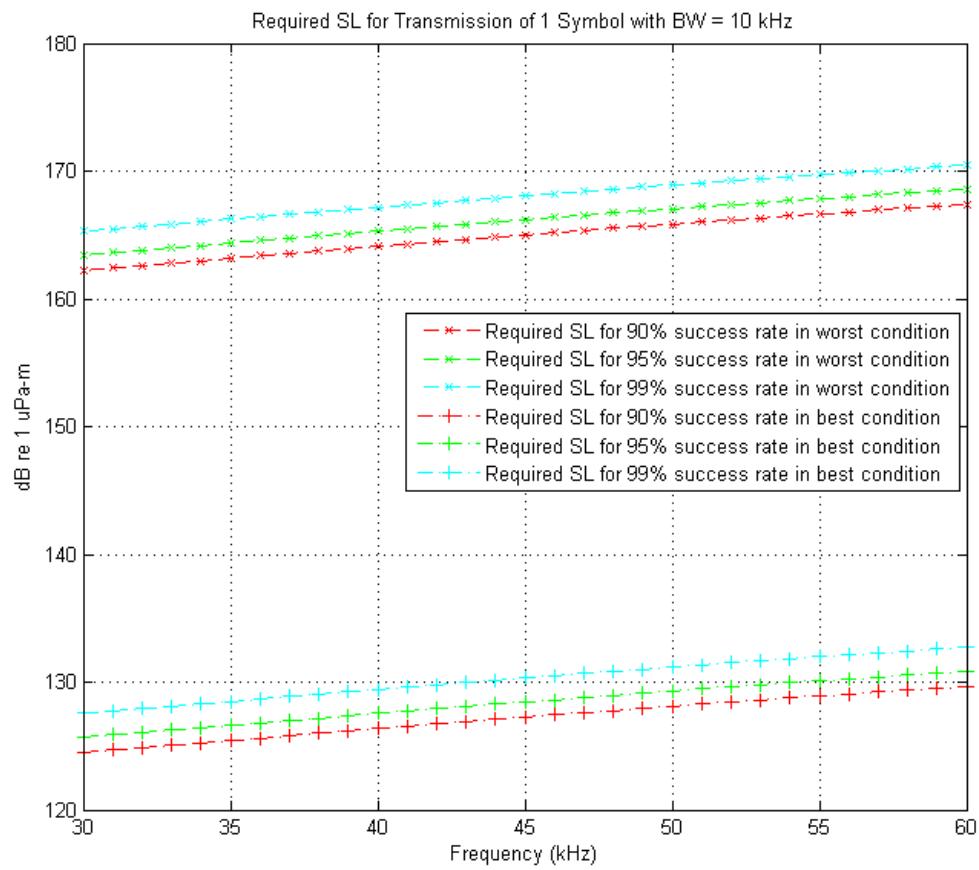
Figure 19. Required narrowband source level for 1 symbol ($SL_{req,\ 1sym}$) for a given bandwidth of 10 kHz, between 30–60 kHz
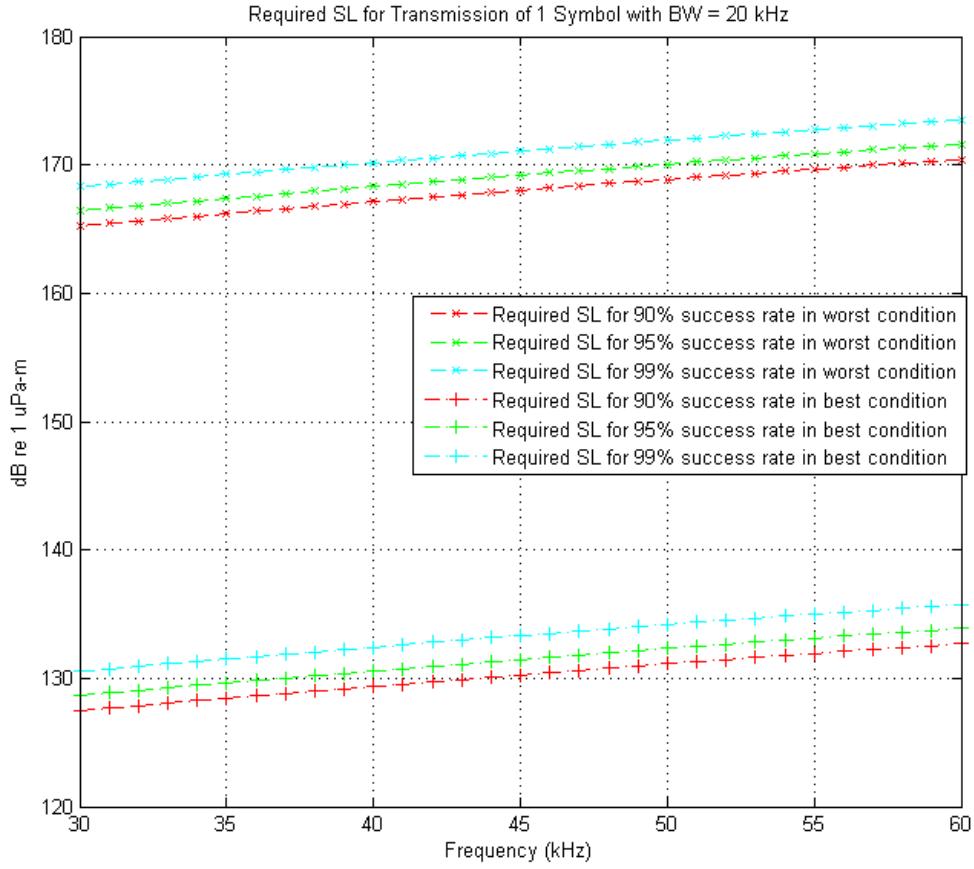
Figure 20.   Required narrowband source level for 1 symbol ($SL_{req, 1sym}$) for a given bandwidth of 20 kHz, between 30–60 kHz

It is assumed that the available operational bandwidth for Seastar modems is between 33 kHz and 55 kHz. For the best (quietest) operating condition, with a spectral bandwidth of 10 kHz, the maximum $SL_{req, 1sym}$ is about 132.0 dB re 1 μPa-m, found at 55 kHz, with 99% success symbol-transmission rate. For the worst (nosiest) operating condition, with a spectral bandwidth of 10 kHz, the maximum $SL_{req, 1sym}$ is about 169.5 dB re 1 μPa-m, found at 55 kHz, with 99% success symbol-transmission rate.

For the best operating (quietest) condition, with a spectral bandwidth of 20 kHz, the maximum $SL_{req, 1sym}$ is about 135.0 dB re 1 μPa-m, found at 55 kHz, with 99% success symbol-transmission rate. For the worst operating (noisiest) condition, with a spectral bandwidth of 20 kHz, the maximum $SL_{req, 1sym}$ is about 172.5 dB re 1 μPa-m,

found at 55 kHz, with 99% success symbol-transmission rate. Table 3 summarizes these maximum $SL_{req,\,1sym}$ required for the best and worst operating conditions.

Table 3.   Maximum $SL_{req,\,1sym}$ required for the best and worst conditions

Spectral Bandwidth	Max. SL_{1sym} for Best Operating Condition (@ 55 kHz with 95% successful 1-bit transmission) (dB re 1 µPa-m)	Max. SL_{1sym} for Worst Operating Condition (@ 55 kHz with 95% successful 1-bit transmission) (dB re 1 µPa-m)
10 kHz	132.0	169.5
20 kHz	135.0	172.5

It can be seen that $SL_{req,\,1sym}$ increases as frequency increases. This is because of the frequency-dependent *TL*. For the best and worst case operating conditions, the difference in $SL_{req,\,1sym}$ is about 38 dB due to the difference between estimated NSL_{min} and NSL_{max}. A symbol-transmission success rate of 99% requires about 2.0 dB greater than a symbol-transmission success rate of 95%, and about 3.0 dB more than for a symbol-transmission success rate of 90%. This is because of the differences in required $SNRL_s$ for each desired symbol-transmission success rate. Lastly, operating with a bandwidth of 20 kHz requires about 3 dB higher source levels than operating with a bandwidth of 10 kHz. This is due to the difference in symbol time duration for the two bandwidths. Since the ratio of symbol duration between the 10 and 20 kHz bandwidths is 2, 10*log(2) accounts for a 3 dB difference in required source level.

This analysis does not account for potential processing gain afforded by forward error correction (FEC). At the cost of reduced information data rate, FEC involves transmission of redundant bits according to a mathematical code. This coding permits a receiver to correct receiver error and to operate successfully at reduced SNR.

IV. TELEDYNE BENTHOS PROTOTYPE SHORT-RANGE ACOUSTIC TELEMETRY MODEM

A. OVERVIEW

The Teledyne Benthos ATM-90X underwater acoustic telemetry modem is a prototype device developed under the sponsorship of the ONR. It is designed for short-range underwater acoustic communication, with an operational frequency band of 33 to 55 kHz. The ATM-90X modem will be used in experimental implementations of the Seastar LAN. It is expected to be capable of transferring a large amount of digital data. By using a 10 kHz or 20 kHz bandwidth, as opposed to the 5 kHz bandwidth in the ATM-885 modem for Seaweb WAN, the ATM-90X modem is expected to achieve maximum raw data transfer rates of 4800 bps or 9600 bps, respectively.

B. SPECIFICATIONS

General specifications and physical characteristics of the ATM-90X modem (Figure 21) are shown in Table 4.
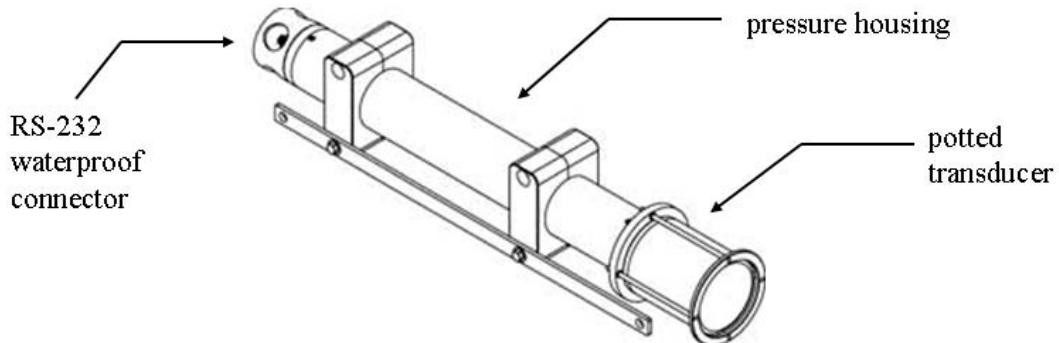
Figure 21. The ATM-90X underwater acoustic modem

Table 4.   General specifications of Teledyne Benthos ATM-90X modem

Type	ATM-90X
Frequency Band	33–55 kHz (VHF)
Bandwidth	2.5 kHz 5 kHz 10 kHz 20 kHz
Data Modulation	Multi-Channel MFSK
Information Bit Rate (for Multi-Channel MFSK)	560–9600 bits/sec
Dimensions	16.0 cm outer diameter 8.6 cm housing (inner) diameter 84 cm long 88 cm long
Average Transmit Power	20 watts at power level 08 (max) at 21 VDC
Battery Capacity	400 watt-hours at power level 08 (max) at 21 VDC
Range	50–500 m

1.   Transducer

The ATM-90X modem uses a ceramic spherical transducer with tapered backing plate to minimize reflection (Figure 22). It is a wide-band transducer that, with factory tuning, has an operating frequency band from about 33 to 55 kHz [5]. The diameter of the transducer sphere is 4.7 cm. The center of the sphere is located approximately 6.3 cm from the end of the pressure housing.
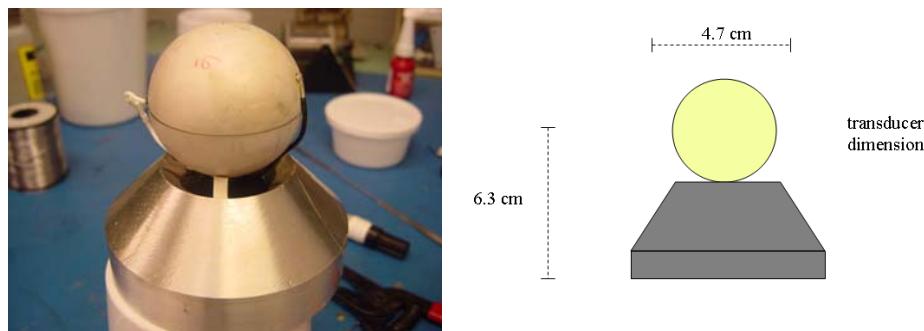
Figure 22.   Spherical transducer used in the ATM-90X modem. From [5]

a.   *Vertical Beam Pattern*

During fabrication, Teledyne Benthos measured the vertical beam pattern of the transducer [5]. The transducer shows a good hemispherical beam pattern (with respect to the forward axis), with reduced radiation in the direction of housing. As shown in Figure 23, at 40 kHz, the vertical beam pattern has its maximum source level of about 174 dB re 1 µPa-m at 0° (top) and has the minimum source level of about 156 dB re 1 µPa-m at 180°(pressure housing). The transducer drive voltage employed to make these measurements is not known.
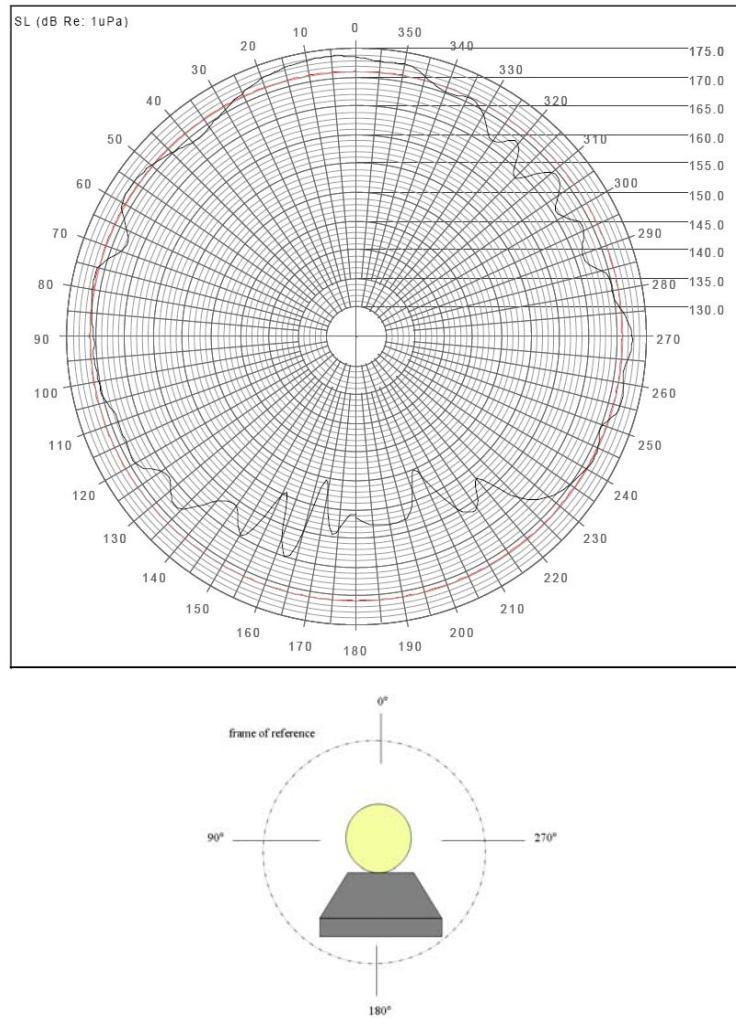
Figure 23.   Vertical beam pattern of the transducer used in the ATM-90X modem. From [5]

b. *Source Level Versus Frequency*

Figure 24 shows the source level of the untuned transducer as a function of frequency, measured at 0°. The transmission resonance is at about 40 kHz with 174 dB re 1 μPa-m. The source level is about 161 dB re 1 μPa-m at 33 kHz and 160 dB re 1 μPa-m at 55 kHz. Again, however, we do not know the voltage used to excite the transducer during this measurement. Nor do we have source level data for the transducer tuned with the matching network ultimately implemented in the modem transmitter.
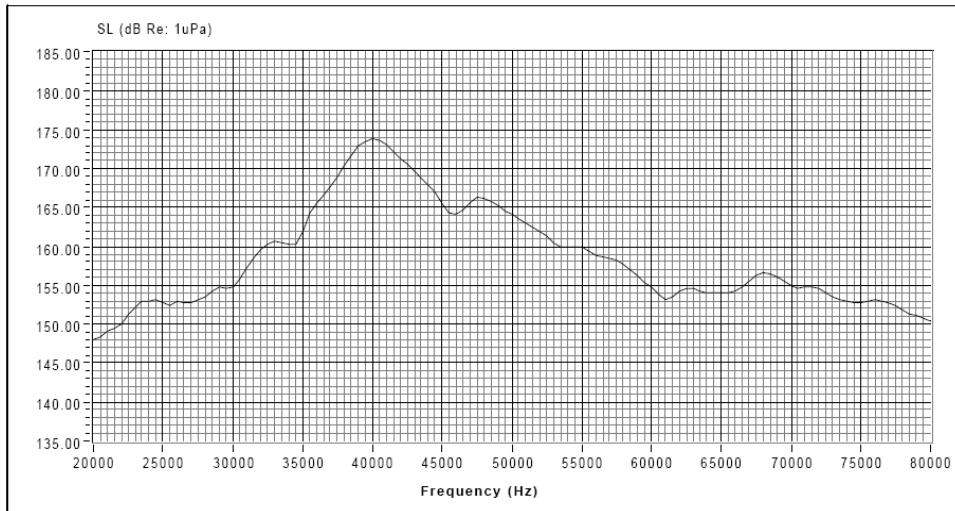
Figure 24.   Source level (untuned) at 0° measured by Teledyne Benthos. From [5]

2.   Maximum Possible Operational Frequency Range

The maximum possible operational frequency range of the ATX-90X modem is from 33 kHz to 55 kHz. There is also a built-in hardware band-pass filter in the receiver module. Its characteristics are consistent with the intended frequency range of 33 to 55 kHz (Figure 25). The band-pass filter has a bandwidth of 25 kHz and the center frequency is at 42.5 kHz. As seen in Figure 25, the characteristic of the band-pass filter shows zero dB gain from 33 to 55 kHz.
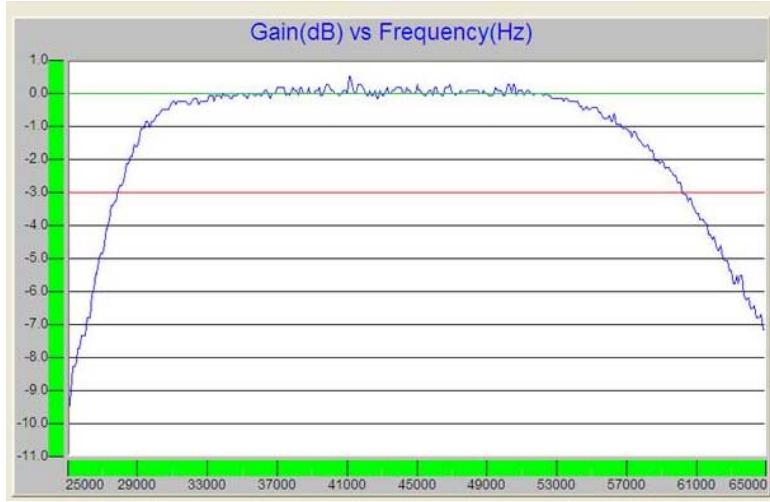
Figure 25.   Characteristic of ATM-90X modem receiver module band pass filter

With the current version of firmware embedded in the ATX-90X modem, the carrier frequency is set at 40 kHz by default. We can select from four available operational spectral bandwidths: 2.5 kHz, 5 kHz, 10 kHz, and 20 kHz.

C.   MODEM SETTINGS

In order to operate the ATM-90X modem with desired operational characteristics, some parameters must be configured. The crucial parameters for operating the modem are data rate, transmit power, operational spectral bandwidth, and carrier frequency. These parameters can be selected by sending commands to a modem via PC or laptop using terminal emulation software (e.g., ProComm Plus). The ATM-90X modem can be directly connected to a PC or laptop using the RS-232 or RS-422 serial interface.

1.   Data Rate

The data rate of the modem is selectable from a range of 140 bits/sec to 2400 bits/sec for multi-channel MFSK modulation, as described in Table 5 [19]. The data rate can be selected by setting the data rate parameter (S Register 4). Since the ATM-90X modem is a prototype device, the command interface has not been fully modified for it. Therefore, the command interface used in the ATM-90X is the same as the one used in

the Seaweb modem. Note that the data rates appearing in Table 5 are for a spectral operational bandwidth of 5 kHz and are to be multiplied by a factor of 2 for a spectral operational bandwidth of 10 kHz or a factor of 4 for a spectral operational bandwidth of 20 kHz, and the times divided by 2 or 4, respectively.

Table 5.   Data rate selection for the ATM-90X modem. From [19]

Setting	Remarks
02	140 bits/s MFSK repeated four times with ½-rate convolutional coding and 25 ms multipath guard period
03	300 bits/s MFSK repeated twice with ½-rate convolutional coding and 25 ms multipath guard period
04	600 bits/s MFSK with ½-rate convolutional coding and 25 ms multipath guard period
05	800 bits/s MFSK with ½-rate convolutional coding and 12.5 ms multipath guard period
06	1066 bits/s MFSK with ½-rate convolutional coding and 3.124 ms multipath guard period
07	1200 bits/s MFSK with ½-rate convolutional coding
08	2400 bits/s MFSK

It can be seen in Table 5 that the data rate depends upon the data reliability methods employed. The greater the protection, the higher the data reliability will be, but the lower will be the data rate [1]. All further analysis in this thesis will assume the uncoded data rate.

2.   Transmit Power

While high transmit power will ensure a high SNR that can support maximum transmission ranges, excessive transmit power is not desirable, as it will also contribute to a high reverberation level that reduces the reliability of short range communication. High transmit power also reduces the operating life of the deployed modem, as it consumes more battery power. The transmit power can be selected by setting the power level

parameter (S Register 6). The available settings are as shown in Table 6, with the values indicating the reduction in power from the maximum level [1].

Table 6.   Power level selection for the ATM-90X modem. From [19]

Setting	Power Level (dB)
00	- 24 dB (Minimum power level)
01	- 21 dB
02	- 18 dB
03	- 15 dB
04	- 12 dB
05	- 09 dB
06	- 06 dB
07	- 03 dB
08	0 dB (Maximum power level)

Note, although the setting is termed "power level," it really determines the maximum voltage magnitude able to be applied to the transducer. The actual values are not known to us. Changing the setting on power level only has an effect down to setting 03 (-15 dB). For the settings 08 to 03, the output power is reduced by 3 dB between each successive setting. For any other settings below setting 03, the output power levels are the same as that of setting 03. This is because, as explained by the manufacturer, the internal power supply is set at its maximum voltage for the maximum power level (08). Then, the voltage is stepped down for each the of lower power levels. But this voltage cannot be reduced below a certain value. At any power levels below -15 dB (03), the power supply voltage is saturated; it cannot go lower. This is verified in Chapter V (D.1.).

3.   Operational Spectral Bandwidth

The operational spectral bandwidth has an effect on the transmit data rate. The wider the bandwidth used, the higher is the data rate.

There are four options of operational spectral bandwidth selection for the ATM-90X modem: 2.5 kHz, 5 kHz, 10 kHz, and 20 kHz. The bandwidth can be selected by setting the bandwidth parameter (S Register 23). The available settings are shown in Table 7.

Table 7.   Spectral bandwidth selection for ATM-90X modem

Setting	Bandwidth
0	10 kHz
1	5 kHz
2	2.5 kHz
3	20 kHz

4.   Carrier Frequency

Carrier frequency is the center frequency of the bandwidth. It can be selected by setting the carrier frequency parameter (S Register 24). The default carrier frequency of the ATM-90X modem is 40 kHz, which corresponds to a value of 234 on S Register 24.

The carrier frequency can be changed by increments of 160 Hz. The formula for calculating the setting of S Register 24 for a desired carrier frequency is given in (4.1–4.3).

$$CarrierFreq = (SettingNumber + 16)*160 \qquad (4.1)$$

$$SettingNumber = \frac{CarrierFreq}{160} - 16 \qquad (4.2)$$

For example, if we want to set the carrier frequency to be 44 kHz, that is:

$$SettingNumber = \frac{44,000}{160} - 16$$
$$SettingNumber = 275 - 16 \qquad (4.3)$$
$$SettingNumber = 259$$

Note that *Setting Number* must be an integer. The "setpriv factory" command and the factory's password are required to change the carrier frequency. Also, it is required to power-cycle the modem before the new carrier frequency setting is in effect.

D. MODEM OPERATIONAL COMMANDS

1. General Commands

The following modem general operational commands (Table 8) were used in this thesis research.

Table 8.   Some commands of the ATM-90X modem that are used in this thesis. From [19]

Command Syntax	Command Name	Result
+++	Online Interrupt	Causes the local modem to go into Command mode.
ATO [Enter]	Online	Causes the local modem to go into Online mode from Command mode.
ATXn [Enter]	Acoustic Link Test	Tests the acoustic link with the modem at address *n*.
ATYn [Enter]	Multiple Bit Rate Test	Tests the acoustic link with the modem at address *n* with transmission of a test packet at multiple bit rates.
AT&W [Enter]	Write	Saves the local modem's S Register settings as the new startup configuration.
ATRn [Enter]	Range	Displays the range from the local modem to the remote modem at address *n*.
ATV [Enter]	Local Battery Voltage	Displays the input power supply voltage and internal temperature of the local modem.

2. Arbitrary Waveform

The ATM-90X can transmit an arbitrary waveform. An arbitrary waveform can be created with the MATLAB 'wavwrite' function.   The waveform must be a stereo WAV file in 16-bit format.   It should be a complex, "based-banded", "analytic" signal (the modem will add the carrier wave frequency to the instantaneous frequency of the arbitrary waveform) [20]. An example of a MATLAB script for creating WAV files is as follows:

```
f = 10000;
t = 0:1:31;
x = 0.9999*exp(i*2*pi*f.*t/40960);
wavwrite([real(x'), imag(x')], 40960,16, 'sine10kHz');
```

wavwrite([(0.9999*ones(1,21))', (zeros(1,21))'], 40960,16, 'ZeroFreq_halfmsec');

The above script is used for creating a 10-kHz sine wave with duration of 0.78 ms and a zero frequency wave with duration of 0.51 ms. There are important key points to note as follows.

First, the sampling rate for creating the WAV file must agree with the selected operating spectral bandwidth. The sampling rate must be 10240 Hz for a 5-kHz bandwidth, 20480 for a 10-kHz bandwidth, and 40960 for 20-kHz bandwidth.

Second, the recorded waveform must be a so-called analytic signal, e.g., $A(t)e^{i\phi(t)}$. This signal will be multiplied by an analytic form of the instantaneous carrier signal, $e^{i2\pi f_c t}$; the real part of the product is transmitted.

Third, the recorded waveform (both real and imaginary parts) is restricted to between ±1. This is a MATLAB limitation when writing floating point values to a WAV file.

Fourth, inputs to the "wavwrite" function must be column vectors.

An arbitrary waveform can be stored in the on-board flash file system on the ATM-90X modem. The on-board flash file system has the total storage capacity of 4 Megabytes [20]. To upload a file onto the modem, the "rx" command (receive via x-modem), specifies the target file name. The following is an example of a file upload [20]:

> *user:4 > rx ffs/myfile*
> *rz: ready to receive ffs/myfile*

To transmit the modulated arbitrary waveform through the modem transmitter, use the "play" command. Following is an example of playing a file [20].

> *user:5 > play ffs/myfile*

V.   PROTOTYPE MODEM PERFORMANCE EVALUATION

We are interested in how the ATM-90X modem will perform as a transmitter. Therefore, the operating performance of the ATM-90X modem was evaluated in terms of its transmit frequency response, vertical beam pattern, and maximum source level. We neglect the horizontal beam pattern because a spherical transducer without any obstacle on the horizontal plane is assumed to produce an omnidirectional horizontal beam pattern. In this chapter, setups and procedures for our evaluation are explained. Results of the evaluation are provided as a conclusion of the chapter.

A.   TEST EQUIPMENT AND FACILITIES

All equipment and facilities used for performing the measurements and evaluation belong to the Physics Department at the Naval Postgraduate School. There are five major categories of equipment and facilities for the tests.

1.   Anechoic Water Tank

The underwater measurements were performed in an anechoic water tank in the basement of Building 232 (Spanagel Hall) at the Naval Postgraduate School. The layout and approximate dimensions of the tank are shown in Figure 26. Note that the lateral dimensions of the tank were measured from the inside tips of the absorbing wall tiles, and depth was measured from the troughs of the absorbing floor tiles to the surface of the water.

.
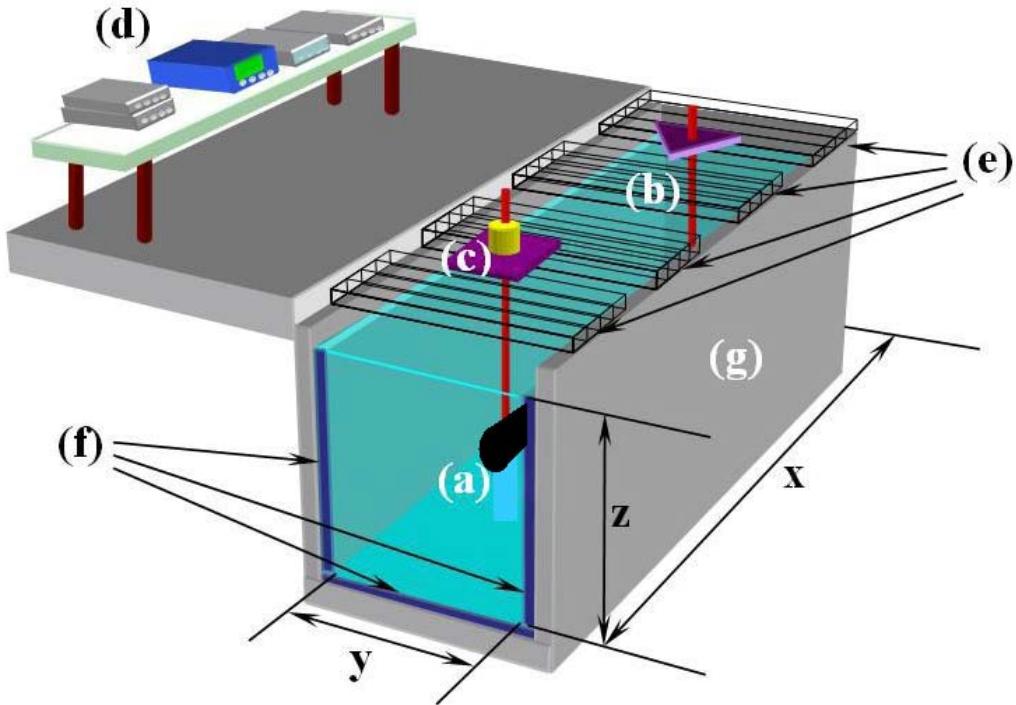
(a) Teledyne Benthos ATM-90X modem;
(b) Receiver hydrophone;
(c) Rotator with azimuthal angle reading;
(d) Equipment bench;
(e) Adjustable floor grids;
(g) Reinforced concrete structure.

x (m)	y (m)	z (m)
7.1	1.6	2.2

Figure 26.   Layout of the anechoic water tank. From [21]

The adjustable floor grids (Figure 26e) were used as a base for supporting the ATM-90X modem and the receiver hydrophone.

2.   Microphones

For preliminary testing in air, a pair of the Brüel & Kjær (B&K) 1/8," type 4138 microphones (Figure 27) were used as signal capturing instruments.   This type of microphone has flatness up to about 100 kHz.

Figure 27.   B&K 4138 microphones

3.   Hydrophones

A pair of B&K hydrophones model 8103 (Figure 28a) was used for the underwater measurements. These have a relatively flat response in the frequency band of interest (less than 3 dB variation from 0 to about 60 kHz), as shown in Figure 28b. A hydrophone with serial number of S/N 1754511 was attached to the top end of the ATM-90X modem as a reference hydrophone. The other hydrophone, S/N 2241680, was placed at a range of 1 m away from the center of the sphere of the transducer as the receiver hydrophone. Figure 29 shows how the reference hydrophone was mounted to the ATM-90X modem.
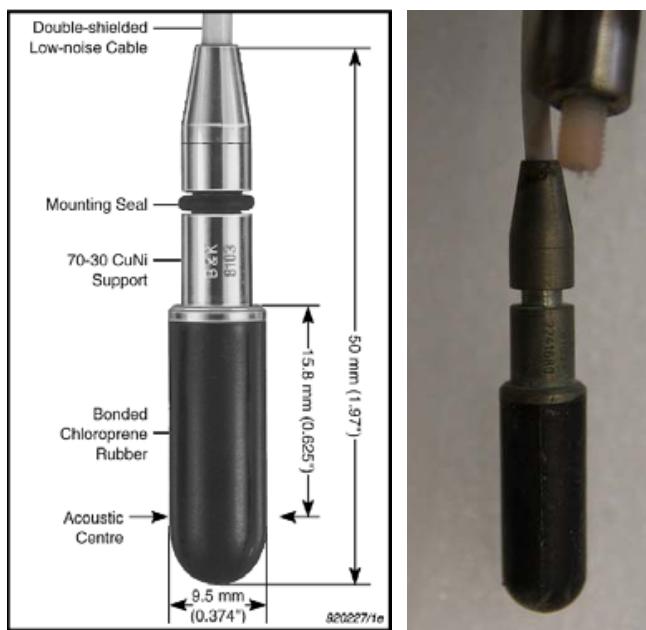
(a) Dimensions of B&K 8103 Hydrophone
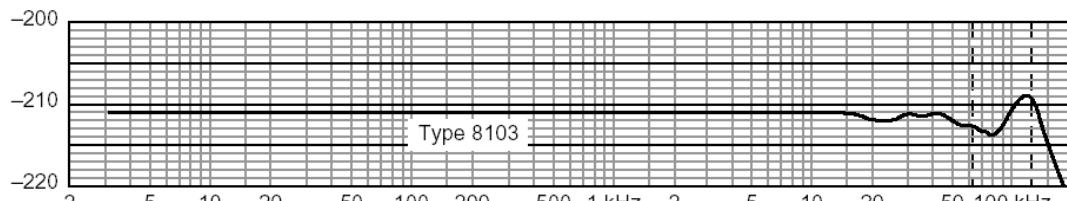
(b) Typical Receiving Voltage sensitivity of the B&K 8103 (dB re 1 V/μPa)

Figure 28.   B&K 8103 hydrophones. From [21]
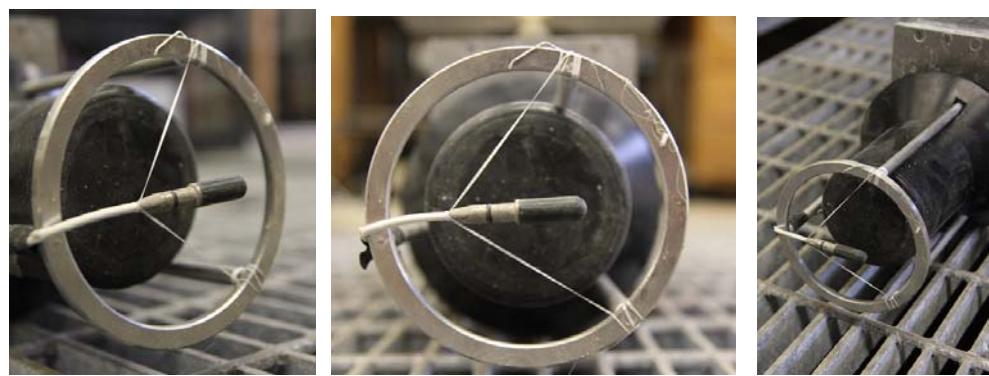
Figure 29.   The reference hydrophone mounted position

4. IOtech Personal DAQ/3000 Series Data Acquisition Box

The IOtech Personal DAQ/3000 Series data acquisition box (Figure 30) is the signal acquisition device used for all measurements. It features a 16-bit/1MHz A/D converter, with 16 analog input channels. For the purpose of our measurements, we used only two analog input channels. Therefore, each channel can have a sampling rate up to 500 kHz. Acquired data can be stored in ASCII format (binary file), MATLAB format (MAT file), or audio format (WAV file).

Figure 30.   IOtech Personnal DAQ/3000 Series data acquisition box

5. Other Equipment and Accessories

Other equipment used for our measurements is as follows:

– B&K Type 2807 Microphone Power Supply

– Stanford Research Systems Model SR560 Low-Noise Preamplifier

– Hewlett Packard (HP) 3314A Function Generator

– Phillips PM 3384 Oscilloscope

– Dell Latitude D620 notebook computers

– MATLAB software (version R2009b)

B. IN AIR TESTS

The purpose of the in air tests was to exercise the ATM-90X modem's functions, and practice using some commands and signal processing techniques. The test was performed in laboratory room 042 in the basement of Building 232 (Spanagel Hall) at the

Naval Postgraduate School. The instruments used for measurements were the two B&K 4138 microphones, a B&K 2807 microphone power supply, two Stanford Research Systems SR560 low-noise preamplifiers, an IOtech Personal DAQ/3000 Series data acquisition box (DAQ), an HP 3314A function generator, a PM 3384 oscilloscope, and two Dell Latitude D620 notebook computers. The setup is shown in Figure 31.
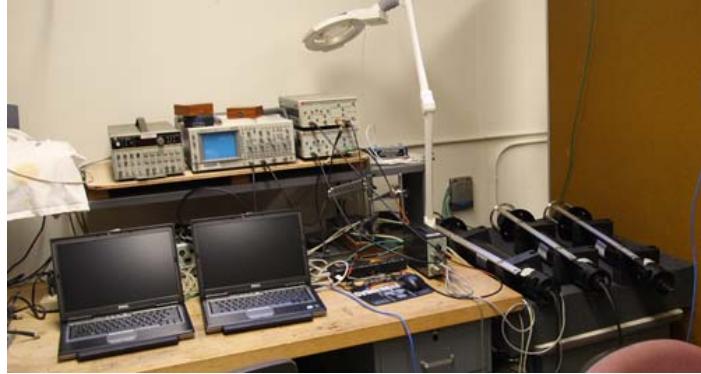
Figure 31.   In air test setup

Before making measurements on transmitted signals in air, we verified that the DAQ functioned correctly. A 45-kHz sinusoidal signal (sine wave) with amplitude 1 V was produced by the function generator and recorded by the DAQ. The spectrogram (time-frequency plot) of the recorded signal from the DAQ showed a single frequency of 45 kHz (Figure 32a). So, the DAQ was verified to work correctly.

Next, we performed a multiple bit-rates test (ATYn command) between two ATM-90X modems that were about 25 cm apart. We performed the test with three different bandwidths (using commands to change S23): 5 kHz, 10 kHz and 20 kHz (S23 = 1, 0, and 3, respectively). Signals were captured with a B&K 4138 microphone and spectrograms were plotted. Figure 32 shows a recorded time series and examples of spectrograms of signals from the multiple bit rates tests.
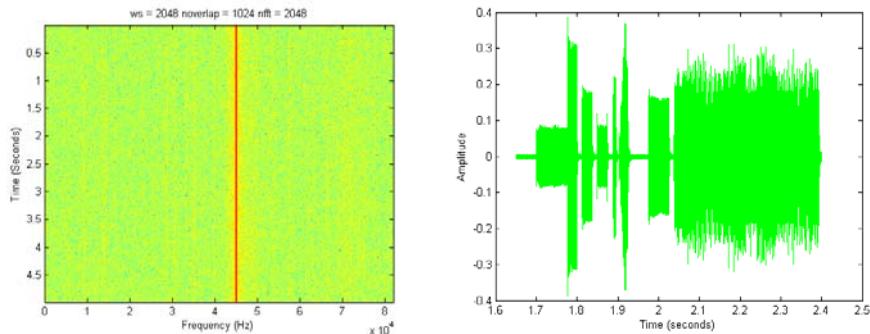
(a) Spectrogram of DAQ verification.   (b) Time series transmit signal.
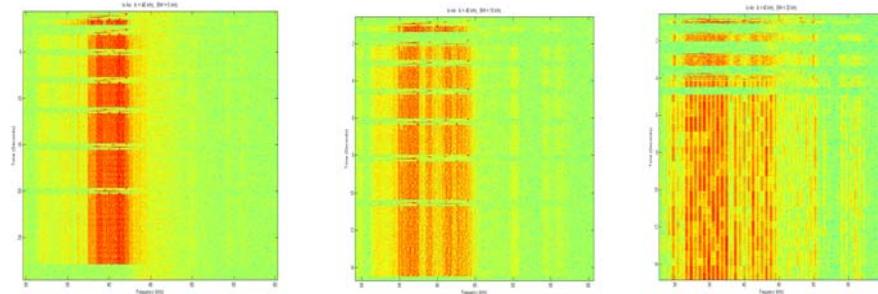
(c) Spectrograms of 5 kHz, 10 kHz and 20 kHz bandwidths, respectively

Figure 32.   Examples of the results from multiple bit rates test in air

The spectrograms show that the setting for the carrier frequency of the ATM-90X modem was at 40 kHz.   In addition, signals were received successfully with the bandwidths of 5 and 10 kHz, but not 20 kHz.

In addition to the multiple-bit-rates test, we recorded two signals with two B&K 4138 microphones, one positioned close to the transmitting modem and the other placed near the receiving modem.   We performed cross correlation between two recorded signals in order to observe multipath effect.   The result was very poor and we could not see the effect of multipath interference.

Lastly, using the procedures described in Chapter IV, we practiced creating some arbitrary waveforms such as sinusoidal waves and hyperbolic frequency modulation (HFM) chirps, and uploaded them into the modem.

From the preliminary multiple-bit-rates test, we developed an understanding of how the ATM-90X modem functions, what its limitations are, and what the expected transmit signals should look like. With this basic knowledge of the ATM-90X modem, we would be able to form the methods and techniques for the underwater measurement, which will be described in next section.

C. IN-WATER MONO FREQUENCY PULSE MEASUREMENTS

In order to obtain the modem characteristics of transmit frequency response, vertical beam pattern, and maximum source level, a mono-frequency pulse technique was implemented for measurements. Details of the technique, setup and how the measurements were performed are described in this section.

1. Setups

The instruments used for in-water mono frequency measurements were two B&K 8103 hydrophones, two Stanford Research Systems SR560 low-noise preamplifiers, an IOtech Personal DAQ/3000 Series data acquisition box (DAQ), a PM 3384 oscilloscope, and a Dell Latitude D620 notebook computer.

Additional accessories, like metallic supports and long cylindrical metallic rods, were also used to position the ATM-90X modem at the desired distance and depth. The layout of the mounted ATM-90X modem for underwater measurements is shown in Figure 33.
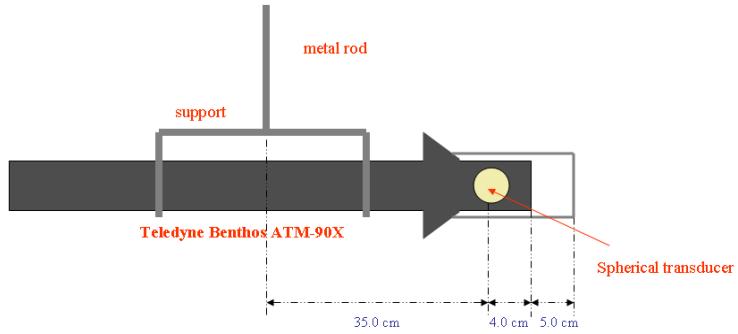
Figure 33.   Layout of the mounted ATM-90X modem

As shown in Figure 34, the ATM-90X modem with attached reference hydrophone and another B&K 8103 hydrophone were both positioned at a depth of 1 m in the anechoic water tank, with a 1 m separation. The modem was controlled by a notebook computer via terminal emulation software (ProComm Plus) using the RS-232 interface. Any given command could be sent to the modem using this method. A notebook computer was also used as a control terminal for the DAQ via a USB interface. Received signals from both hydrophones were amplified by SR560 preamplifiers. A PM 3384 oscilloscope was used to observe and perform real-time analysis on characteristics of the amplified signal. Both amplified signals were passed to the DAQ for digital sampling. Finally, these finally amplified and digitized signals were sent to the notebook for storage and later analysis.

(a) Equipment bench.
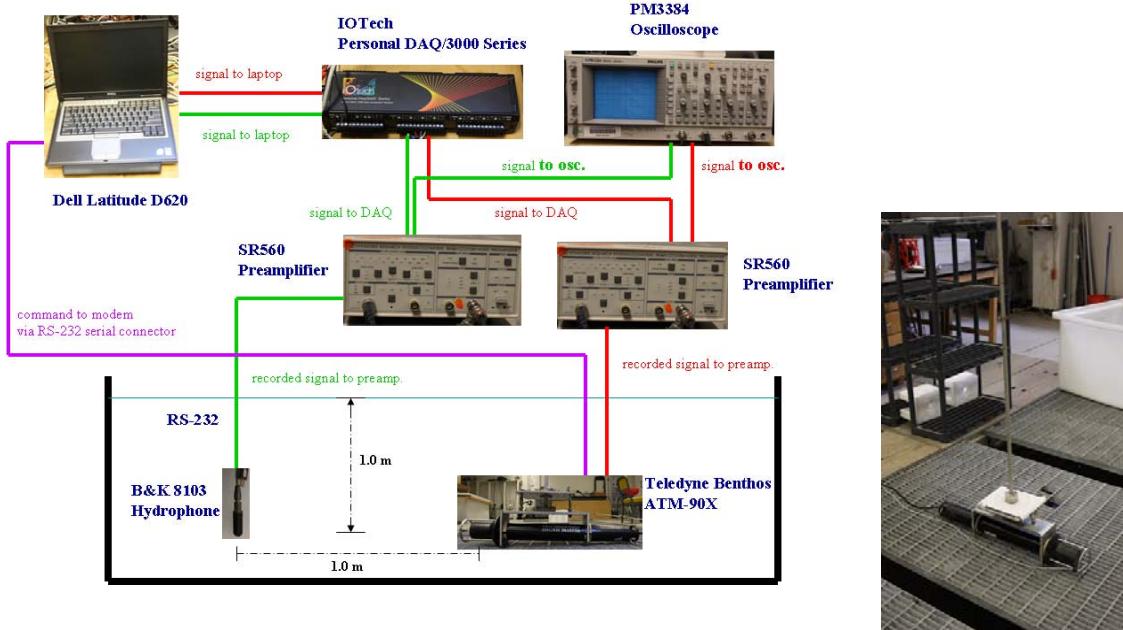
(b) Diagram of setups.

(c) Mounted modem.

Figure 34.   Setups for measurements

The general setup used for all measurement was as follows. For the ATM-90X, the spectral bandwidth (S23) was set at 20 kHz. Amplifier gain for the SR560 preamplifier was set to 20. The sampling rate of the DAQ was about 328.77 kHz. This would give between 6 to 11 sampling points per cycle between the frequencies of 30 to 60 kHz. The total time record length for all recorded data sets was 5 s.

2.   In-Water Measurements and Signal Processing Technique

In general, a measurement of a transducer's characteristics, such as frequency response, beam pattern, source level, etc., is obtained from a tone burst transmitted by a transducer. If we had direct access to the modem's transducer element, a pulse signal

with desired frequency and waveform could be input to and transmitted from the transducer. Then, the transmitted signal could be captured by using a hydrophone positioned at a range of 1 m from the center of a transducer to obtain the transmitted voltage sensitivity (TVR) [22].

However, in the case of the ATM-90X modem, we are unable to directly energize the transducer with our chosen pulse signal. We must create all desired transmit signals by "playing" a suitable arbitrary waveform (WAV) file. And, as mentioned previously, the actual signal transmitted is the arbitrary waveform file signal, frequency-shifted by the carrier frequency. Therefore, in order to perform the mono frequency pulse-measurement, we have to find a technique that makes the ATM-90X transmit a single pulse of our desired frequency.

Based on the specifications and functions of the ATM-90X modem, any arbitrary waveform can be created, uploaded and played (transmitted). We can also specify an arbitrary carrier frequency (S24). After performing detailed study and experiments on these capabilities, we decided that if a zero frequency pulse ("1") of a certain time duration is used an input WAV file, the transmit signal from the modem is a pulse of the same duration, at the carrier frequency. Therefore, we can make the modem transmit a desired single frequency pulse by creating a zero frequency pulse. Then, the pulse is uploaded to and transmitted by the modem with a selected carrier frequency. This scheme was used throughout the measurements.

a. Zero Frequency Pulse

For the mono frequency pulse measurement, we created a zero frequency signal (WAV file) with a value of 1+j0 (maximum value allowed by the "wavwrite" function in MATLAB) and a duration of about 0.5 ms. There were between 15 (at 30 kHz) to 30 (at 60 kHz) cycles per pulse with the pulse duration of 0.5 ms. The zero frequency was chosen to ensure that the modulated signal has the same frequency as the specified carrier frequency. Thus, the transmit signal resulting from the modulation was a mono frequency pulse with the same frequency as the carrier and the same duration as

that of the zero frequency input signal. By implementing a zero frequency signal as the input, we were able to make a measurement on every allowable carrier frequency in the bandwidth of our interest.

The pulse duration of 0.5 ms was selected to avoid an interference effect from the surface reflection. In the geometry of our test setup, both the ATM-90X modem and the receiver hydrophone were in the anechoic water tank at a depth of 1 m and the receiver hydrophone was positioned at a range of 1 m from the ATM -90X modem. Even though reflections from the sides and bottom of the tank were negligible, interference due to the surface reflection was expected.

As illustrated in Figure 35, the path difference between direct path and reflected path is $\sqrt{5}-1=1.236$ m. With the assumption that sound speed in the water is 1480 m/s, the difference in time travel from a source to receiver between the direct path and reflected path is about 0.8 ms. In other words, the signal from direct path would arrive at the receiver hydrophone approximately 0.8 ms before the signal from the reflected path. Therefore, with a signal duration of 0.5 ms, we could be certain that, within the first 0.5 ms of the recorded signal, there would not be interference due to surface reflection.
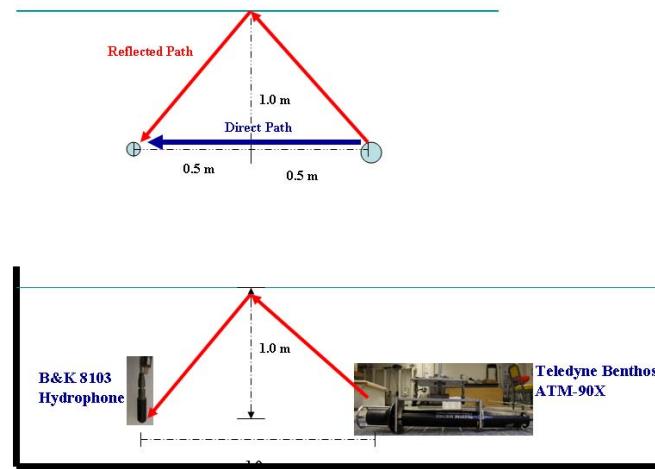
Figure 35.   Surface reflection interference

Therefore, a short pulse of zero frequency was used as an input arbitrary waveform to ensure the fidelity of the measurements.

b. Windowed Time Signals

Since we used two B&K 8103 hydrophones to record signals, we obtained two channels of time series data for each test transmission. The first was a time series captured by the reference hydrophone attached to the end of the ATM-90X modem. The second was a time series captured by the receiver hydrophone at a range of 1 m from the modem transducer. Figures 36a and 36b show an example reference signal and received signal, respectively. The small amplitude signal commencing at about 1.2 ms in the reference hydrophone signal, and the medium amplitude signal commencing at about 0.8 ms in the received hydrophone signal are first reflections from the air-water interface. Reflections from the side and bottom boundaries, which are covered with anechoic tiles, are not visible.
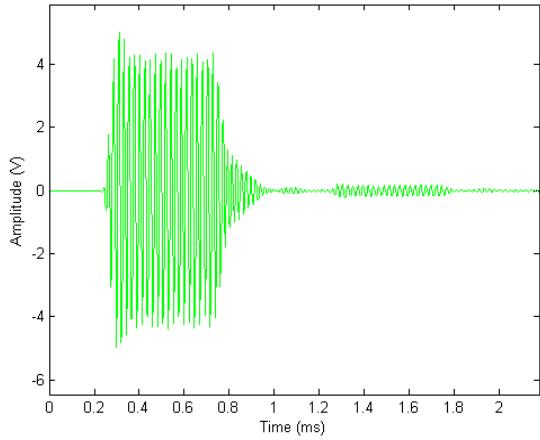
(a) Reference signal
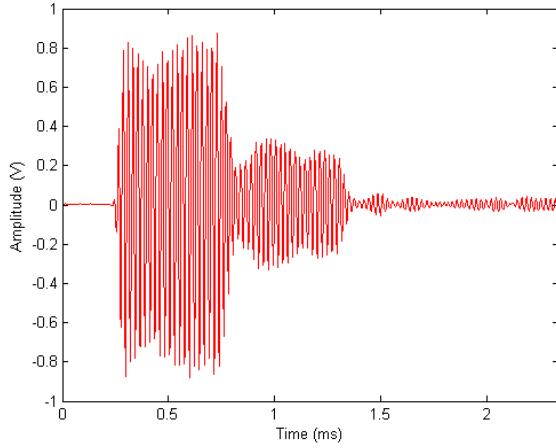
(b) Received signal

Figure 36.   Recorded time series data

Procedures for producing windowed time signals from the recorded data for each channel are as follows. First of all, each recorded time series had duration of 5.0 s, while we were interested in only our transmit signal, which was only 0.5 ms long. We began by performing a Hilbert transform on the recorded time signals of both the reference and received channels. Then, the onset of the reference and received signals were determined from examination of the absolute value of the Hilbert-transformed data, which produces the envelope of the data. We set a threshold of 10% of the maximum value of the absolute value of Hilbert transform (Figure 37). We declared that signals start when they reach this threshold.

(a) Reference signal (b) Received signal
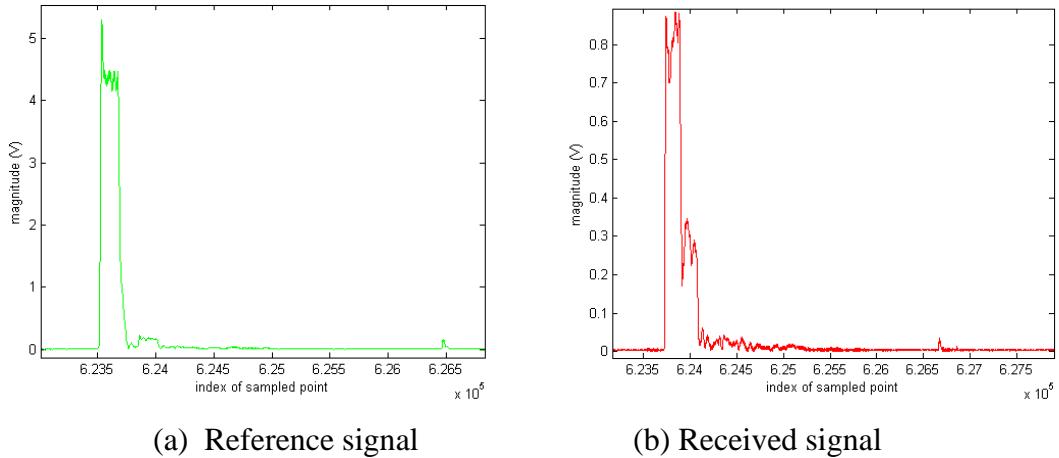
Figure 37.   Absolute values of Hilbert transform of recorded signals

After onset of the signals, the waveforms usually exhibited transient behavior for about 0.2 ms. This transient behavior would not affect the ability to successfully communicate a symbol because, for 20 kHz bandwidth, for example, in multi-channel MFSK, the time duration of symbol transmission is 6.25 ms. A portion of 0.2 ms is only about 3% of the whole symbol transmission duration. For our analysis, we windowed the reference and received signals for a duration of 0.3 ms, beginning 0.2 ms after the declared onset. This was done to eliminate all but direct-path signals. There were sufficient number of cycles, between 9 (at 30 kHz) to 18 (at 60 kHz) cycles per pulse with the pulse duration of 0.3 ms. These were referred to as "windowed-reference signal" and "windowed-received signal." Figure 38 shows examples of windowed-reference and windowed-received signals. Note that both windowed-reference and windowed-received signals were taken with proper delay so that they were approximately from the same portions of the transmit signal. In other words, the phase rotation due to the distance between reference and receiver hydrophones was excluded.
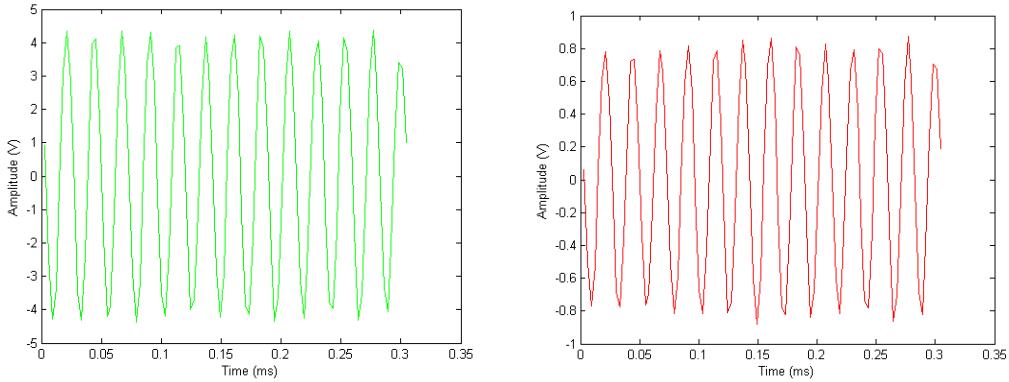
Figure 38.   Left: Windowed-reference signal; Right: Windowed-received signal

The windowed signals were, then, used for two types of analysis: transmit frequency response and vertical beam pattern.

3.   Measurements

a.   Transmit Frequency Response (Source Level)

In this measurement, 30 different carrier frequencies between 30 kHz and 60 kHz, at intervals of approximately 1 kHz, were selected for the measurement.   For each carrier frequency, the modulated signal was transmitted and recorded for three transmit power level settings: 08 (maximum level), 04 (-12 dB), and 00 (-24dB).

Later, we chose three particular frequencies of interest; 33.12 kHz, 43.04 kHz, and 53.12 kHz. These frequencies correspond to candidates for lower cutoff, carrier frequency and upper cutoff for a bandwidth of 20 kHz.   At these three frequencies of interest, we measured the source level for each power level settings, from 08 (maximum level) to 00 (-24 dB).

For each transmitted frequency and power setting, the source level was obtained from the windowed-received signal as follows.   A Hilbert transform was performed on the windowed-received signal.   Then, the average amplitude of the windowed-received signal was obtained by taking the average of the absolute values of the Hilbert transformed signal (Figure 39).
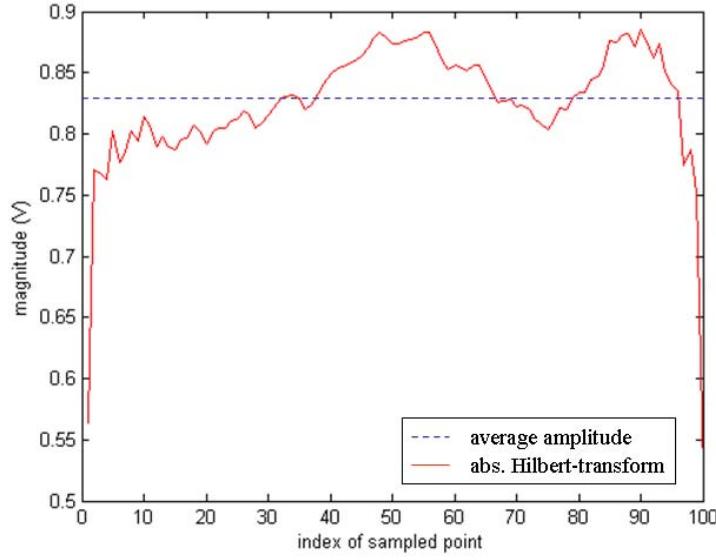
Figure 39.   Absolute values of Hilbert transform of windowed- received signal

The result was the average amplitude of the signal in volts measured at the range of 1 m from the center of the transducer. This average value was used to compute the source level (*SL)* in dB re 1 μPa at 1 m , which is given by:

$$SL_{each\ frequency} = 20\log(\frac{avg}{\sqrt{2}} \times \frac{1}{m0} \times \frac{1}{Gain} \times \frac{1}{P_{ref}}) \qquad \text{dB re 1 μPa-m} \qquad (5.1)$$

where

avg: Average amplitude of the windowed and Hilbert-transformed signal (V)

*m*0:   Open circuit sensitivity for B&K 8103 hydrophone (V/Pa)

Gain: Gain of SR560 low-noise preamplifier

P_{ref}:   Reference pressure acoustic pressure for water (1 μPa)

For our case, m0 for B&K 8103, S/N 2241680, is 26.0 μV/Pa and Gain is 20.

b.   *Vertical Beam Pattern*

After the transmit frequency response for three power levels was measured, we again chose three particular frequencies of interest: 33.12 kHz, 43.04 kHz,

63

and 53.12 kHz. Therefore, the transmit signals were 0.5 ms pulses at frequencies 33.12 kHz, 43.04 kHz, and 53.12 kHz.

For this directivity measurement, the receiver hydrophone was placed at a distance 1 m away from the center of the transducer. The measurements were made at intervals of 10°, from -180° to +180°. For the measurement at each angle, instead of moving the reference hydrophone to a desired angle relative to the ATM-90X modem, we fixed the reference hydrophone and rotated the ATM-90X modem to the desired angle (Figure 40). In order to ensure the distance to the receiver hydrophone remained 1 m after rotating, the position of the ATM-90X modem was adjusted laterally, whereas the receiver hydrophone was used as a center of reference. For example, for the measurement at 0° (top), we aligned the top of the modem directly toward the receiver hydrophone. Therefore, the modem was positioned at the center. As the measurements went toward ± 90° (broadsides), position of the modem was shifted laterally away from the centerline reference so that the center of the transducer was positioned at a desired angle and was always 1 m away from the reference hydrophone. For each test frequency, the measurements were made for power level settings: 08 (maximum power) and 04 (-12 dB).
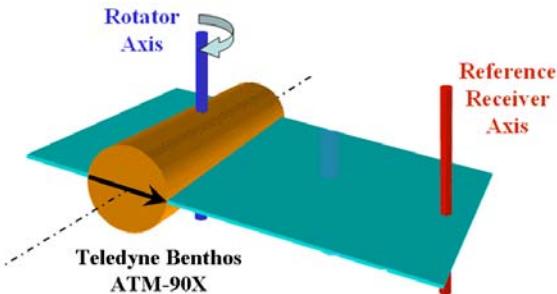
Figure 40.   Beam pattern measurement. From [21]

For the vertical beam pattern measurement, an autocorrelation was performed on the windowed-reference signal and a cross-correlation was performed

between the windowed-received signal and the windowed-reference signal. The results of the autocorrelation, cross-correlation, and a comparison between them are shown in Figure 41.

(a) Autocorrelation.   (b) Cross-correlation.

(c) Comparison between auto and cross correlations.
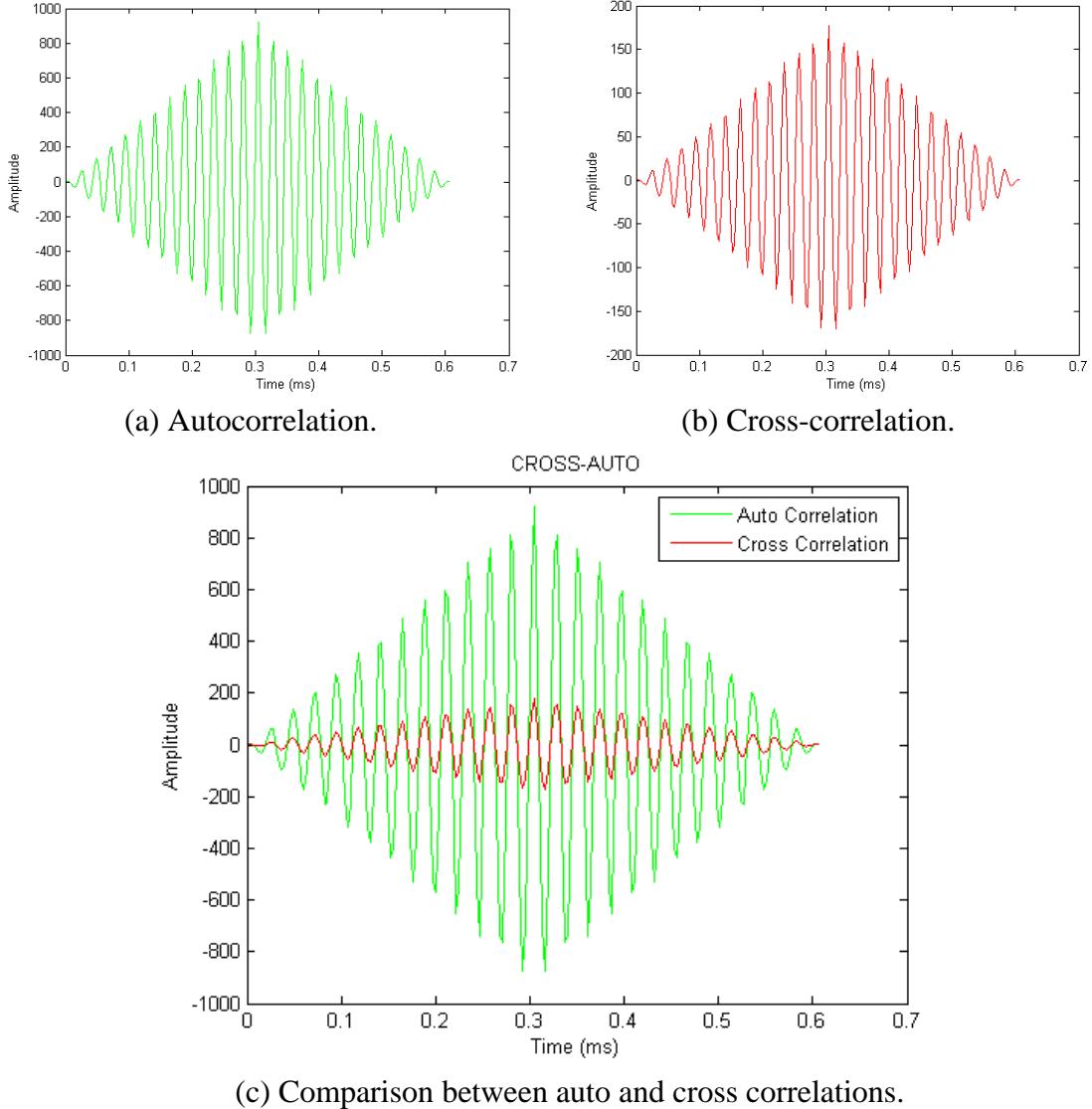
Figure 41.   Auto and Cross Correlations of the windowed-received and windowed reference signals

After the auto and cross correlations were obtained, we divided maximum value of the absolute value of the cross correlation by the maximum value of the autocorrelation to get the un-normalized axial (vertical) directional factor, called $H_{unnorm}(\theta)$. The formula is given by:

65

$$H_{unnorm}(\theta) = \frac{|R_{xy}|}{R_{xx}} \tag{5.2}$$

where

$H_{unnorm}(\theta)$:   Un-normalized, axial directional factor for each angle

R_{xy}:   Cross correlation

R_{xx}:   Autocorrelation

       This factor ($H_{unnorm}(\theta)$) is an estimate of the gain (transfer function) magnitude from reference to receiver hydrophones. Then, the peak maximum value of all measured $H_{unnorm}(\theta)$ (from 0° to 350°) was identified. All un-normalized, axial directional factors were then normalized by the peak maximum value to obtain the normalized axial directional factor $H(\theta)$. The beam pattern in dB is given by:

$$b(\theta) = 20\log(H(\theta)) \quad dB \tag{5.3}$$

c.   *Linearity*

      The purpose of this measurement was to verify the linearity of the internal amplifier of the ATM-90X modem. We created a signal that is the superposition of 32 sinusoidal waves whose frequencies correspond to the centers of 32 4-ary FSK channels, ranging from 33 kHz to 53 kHz. The component sine waves all had the same amplitude. The superimposed signal was, then, normalized so its maximum possible amplitude was 1. Each component, then, had the amplitude of 1/32 (because there were moments when all components interfered by completely constructively). A zero-frequency signal with amplitude of 1 was also created. The duration of both signals was 3.125 ms. Both signals were uploaded into the ATM-90X modem, played and recorded by the reference hydrophone.

      The concept of this test is that, when the modem transmits the superpositioned sinusoidal signal, it is equivalent to transmitting 32 symbols across the bandwidth. This test signal is representative of a multi-channel 4-ary FSK symbol package transmission. Whereas, the zero-frequency signal is equivalent to transmitting 1 symbol using the entire SL, with the power concentrated into one symbol only.

The formula used to create the WAV file of the superimposed sinusoidal signal that we uploaded into the ATM-90X modem is given by:

$$wav = \frac{1}{32} \sum_{i=1}^{32} (\sin 2\pi f_i t - i \cos 2\pi f_i t) \qquad (5.4)$$

where "wav" is the superimposed sinusoidal signal. The values of f_i were from -10560 Hz to +10560 Hz with the increment of 640 Hz. The inverse of this frequency spacing is 1.5625 ms. A time record signal of duration equal to an integer multiple of 1.5625 ms will ensure the orthogonality between each frequency component (in that the "overlap time integral" between components will be zero). In our case, the duration of the time record signal was 3.125 ms which was twice of the period 1.5625 ms. Therefore, each frequency component was orthogonal to each other over the time record of 3.125 ms.

$$wav = \frac{1}{32} \sum_{i=1}^{32} (\sin 2\pi f_i t - i \cos 2\pi f_i t) = \frac{-1}{32} \sum_{i=1}^{32} (\sin \omega_i t - i \cos \omega_i t) \qquad (5.5)$$

$$wav = \frac{-j}{32} \sum_{i=1}^{32} e^{j\omega_i t} = \frac{1}{32} \sum_{i=1}^{32} e^{j(\omega_i t - \frac{\pi}{2})} \qquad (5.6)$$

The carrier frequency analytic signal is given by:

$$carr = e^{j\omega_c t} \qquad (5.7)$$

If $y(t)$ is the transmitted signal, $y(t)$ is the real part of "*carr*" multiplied with "*wav*," which is:

$$y(t) = \text{Re}[carr * wav] \qquad (5.8)$$

$$y(t) = \text{Re}[\frac{-j}{32} \sum_{i=1}^{32} e^{j(\omega_c + \omega_i)t}] \qquad (5.9)$$

$$y(t) = \frac{1}{32} \sum_{i=1}^{32} \sin(\omega_c + \omega_i)t \qquad (5.10)$$

The energy of *y(t)* is:

$$\varepsilon[y(t)] = \int_0^T (\frac{1}{32})^2 (\sum_{i=1}^{32} \sin(\omega_c + \omega_i)t)(\sum_{j=1}^{32} \sin(\omega_c + \omega_j)t)dt \qquad (5.11)$$

By the orthogonality of each sine wave component by design, the energy can be expressed as:

$$\varepsilon[y(t)] = \int_0^T (\frac{1}{32})^2 (\sum_{i=1}^{32} \sin^2(\omega_c + \omega_i)t)dt \qquad (5.12)$$

$$\varepsilon[y(t)] = (\frac{32}{32^2})(\frac{T}{2}) = (\frac{1}{32})(\frac{T}{2}) = \frac{1}{32} \text{ of single tone energy} \qquad (5.13)$$

The zero-frequency (single tone) signal $z(t)$ is given by:

$$z(t) = \sin 2\pi f_c t = \sin \omega_c t \qquad (5.14)$$

The energy of the $z(t)$ is given by:

$$\varepsilon[z(t)] = \int_0^T \sin^2 \omega_c t dt = \frac{T}{2} \qquad (5.15)$$

We get the energy of the transmit signal of the superpositioned sinusoidal signal as $\frac{1}{32}$ of single tone energy. The energy of the transmitted zero-frequency WAV file (carrier frequency only) is $\frac{T}{2}$. The relative root mean square (rms) value the superpositioned sinusoidal signal and zero frequency signal is a square root of the ratio between the energy of both signals, which is $\frac{1}{\sqrt{32}}$, or 0.1768 in our case.

So, if the internal amplifier behaves linearly, the relative rms value of the two signals will be the same as for the WAV files.

From recorded signals captured by the hydrophone (Figure 42), the square root of the ratio of energy between the superimposed signal and the zero-frequency signal is 0.1787. This is very close to the theoretical ratio 0.1768 of those WAV files. Therefore, the ATM-90X modem displays acceptable linearity in the internal amplifier.
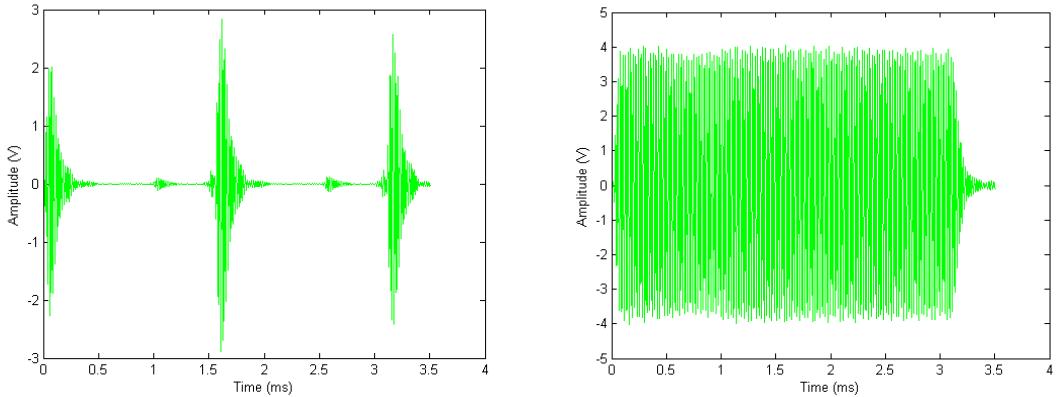
Figure 42.　　Left: recorded superpositioned sinusoidal signal.
Right: recorded zero-frequency signal

Furthermore, transmitting superpositioned sinusoidal signal is equivalent to transmitting 32 symbols across the bandwidth, while transmitting the zero-frequency signal is equivalent to transmitting 1 symbol using the entire *SL*. Thus, the energy per symbol when 32 symbols are being transmitted is $(\dfrac{1}{32})^2$ that of a single symbol with the same *SL* when only one symbol is using the entire *SL*.

Therefore, in terms of dBs, the energy per symbol when transmitting 32 symbols across the bandwidth is less than energy per symbol when transmitting a single symbol using entire bandwidth by:

$$10\log(32^2) = 20\log(32) = 30 \quad \text{dB} \tag{5.16}$$

D.　　RESULTS

1.　　Transmit Frequency Response

Figure 43 shows measured transmit frequency responses (source levels) for three power levels: maximum (08), -12 dB (04), and -24 dB (00) levels, from 25 to 62 kHz. It also shows the measurement of source level (*SL*) for each power level from 00 to 08 at frequencies 33, 43, and 53 kHz.
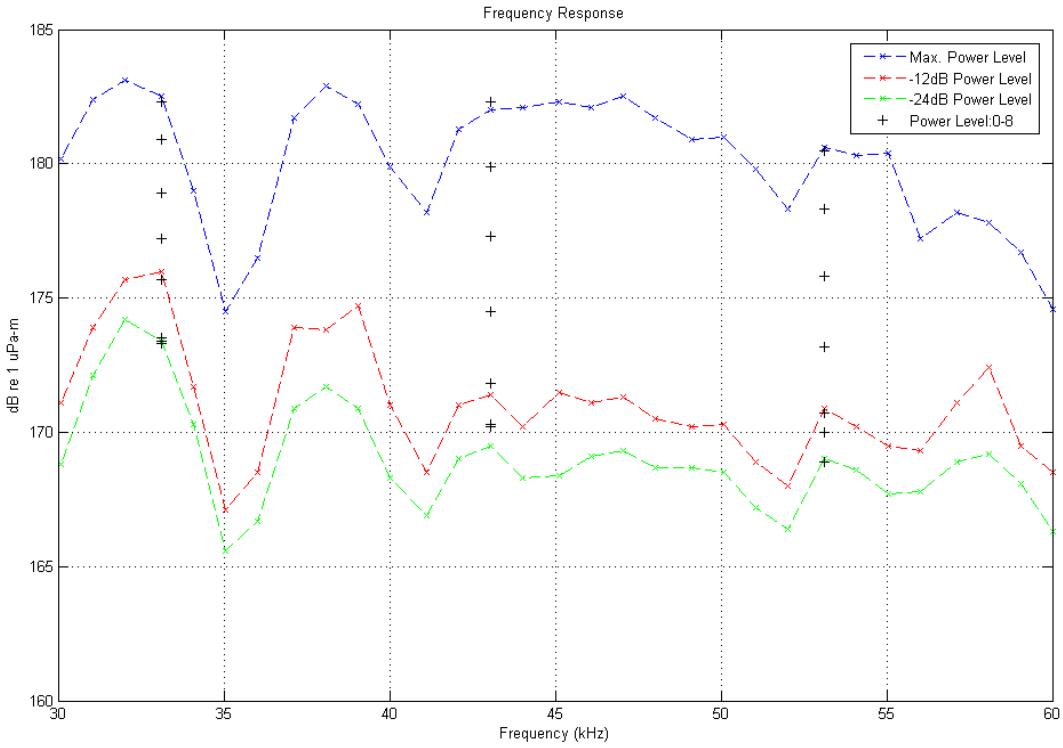
Figure 43.   Transmit frequency response

For the maximum power level (08 level), the maximum *SL* (resonance) is about 183 dB re 1μPa-m at 38 kHz. The transmit frequency response does not show acceptable flatness (within 3 dB from the maximum response) from 33 kHz to 55 kHz. There is one major null at 35 kHz where the *SL* is about 8.5 dB lower than the maximum response. There are two additional nulls at 41 and 52 kHz, where the *SL* are 5 dB lower than the maximum SL.

For power levels of -12 dB (04 level) and -24 dB (00 level), the transmit frequency responses show the same pattern as the one measured for maximum power level. The *SL* for the -12 dB power level is approximately 10 dB lower than for the maximum power level. The response for the -24 dB power level is approximately 12 dB lower than for the maximum power level.

Source level measurements made at 33, 43, and 53 kHz at all power level settings, reveal that power levels 00 to 03 produce approximately the same transmit *SL*. Power

70

levels 04 to 08 produce *SLs* consistent with those expected, base upon a 3 dB difference between adjacent power level settings. These results verified the transmit power setting explained in Chapter IV.

2.   Maximum Source Level

The maximum SL is observed at a vertical (axial) angle of 0°.

In practical operation, modems will be moored in an upright configuration at approximately the same depth, very close to the bottom. The useful radiation angles can be expected to correspond to the broadside of the modem rather than the top. Therefore, our metric for useful source level needs to be the broadside value. The level at the broadside is on average about 5 dB lower than on axis. So, the *SL* should be decreased by 5 dB for all frequencies, to account for the difference in levels between the 0° and the 90° directions of the modem. The broadside maximum source level (SL_{max}) of the ATM-90X modem is shown in Figure 44.
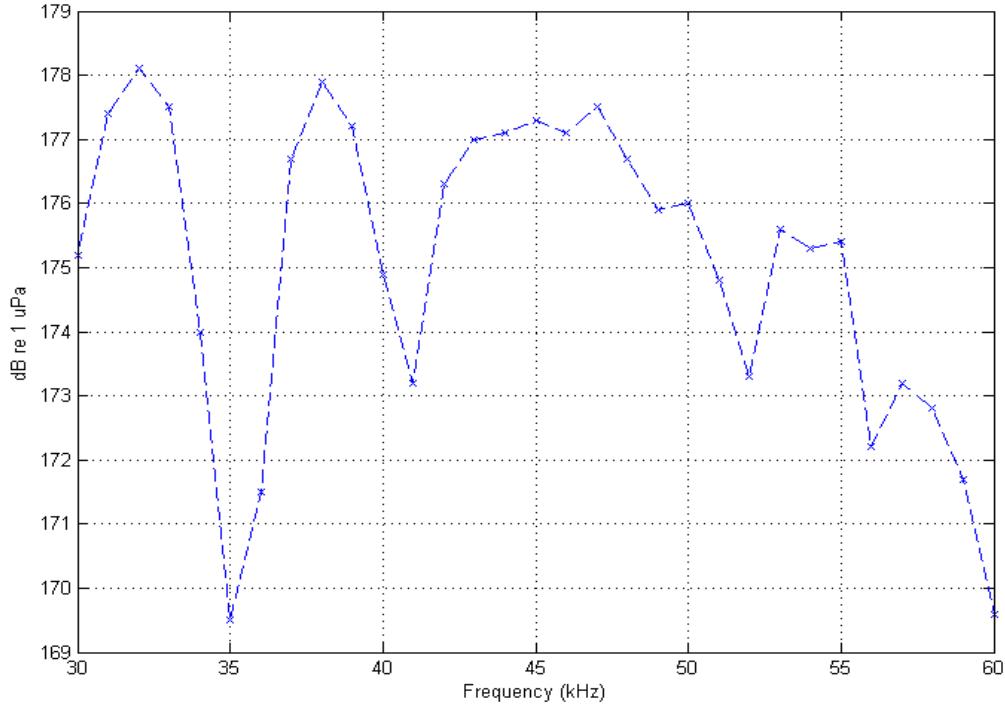
Figure 44.   Broadside maximum source level (SL_{max}) of the ATM-90X modem

3. Vertical (Axial) Beam Pattern

Figure 45 shows the normalized beam pattern measured for the maximum power level (08) at frequencies 33, 43, and 53 kHz. All beam patterns exhibit a good omnidirectionality in the upper hemisphere. The patterns have maxima at 0° (top of the modem) and drop to the average of about -5 dB at ±90° (broadside of the modem). They have nulls of about -25 to -35 dB at 180° (pressure housing).
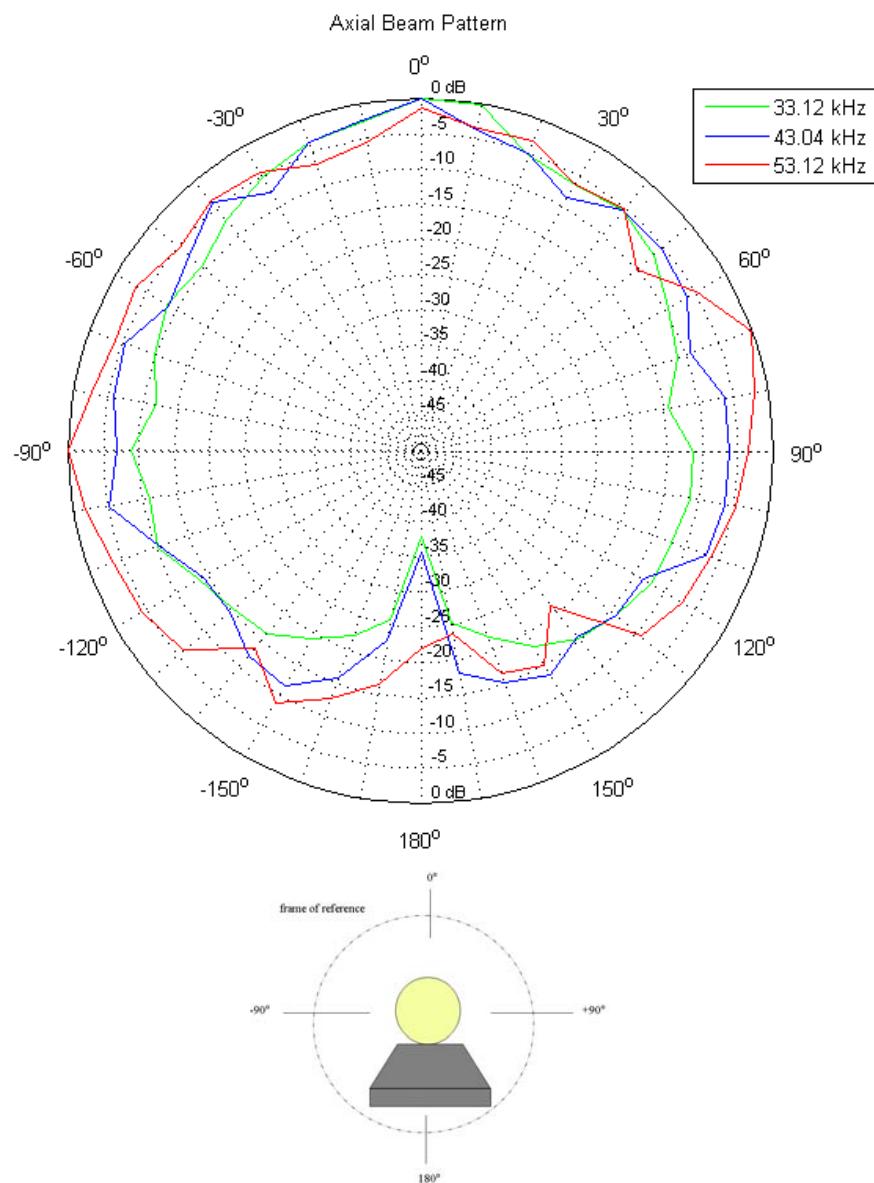
Figure 45.   Normalized vertical (axial) beam pattern
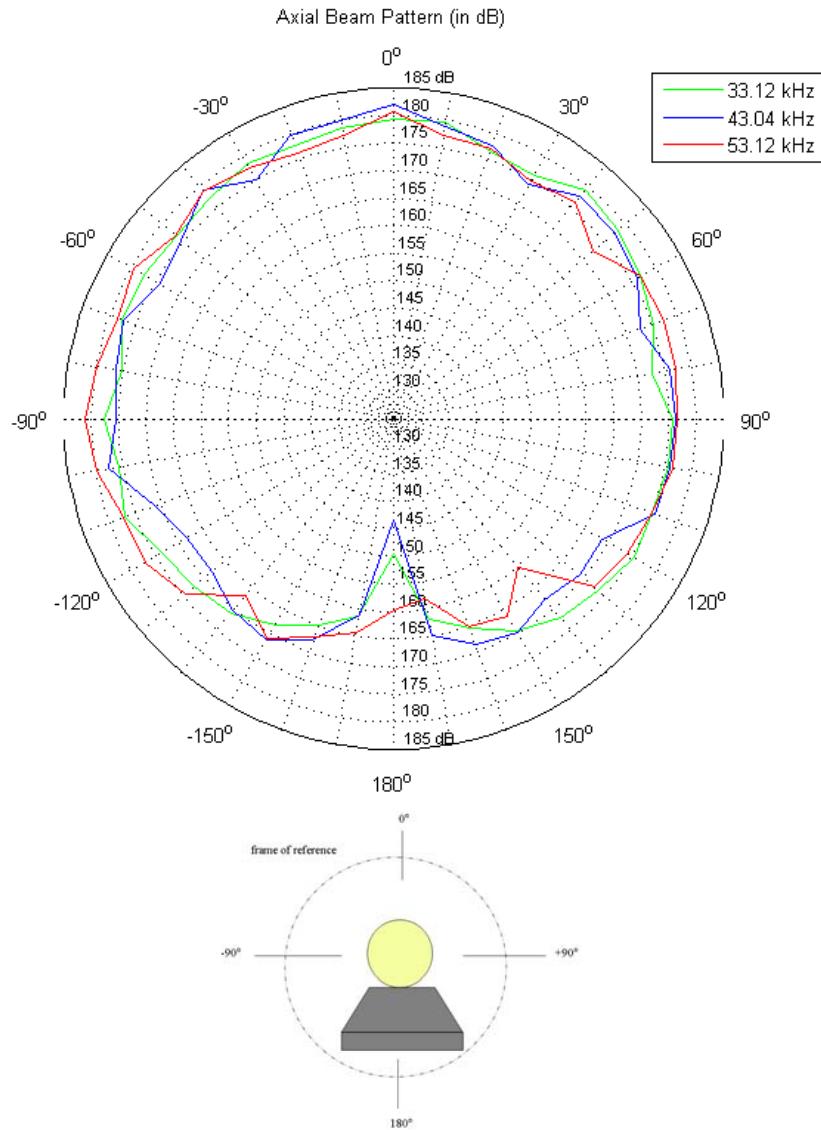
Figure 46.   NPS-measured source level in the vertical plane
at 33, 43, 53, and 53 kHz

By comparison with the vertical (axial) beam pattern of the transducer at 40 kHz measured by Teledyne Benthos (Figure 47), there is similarity between our measured patterns at 33, 43, and 53 kHz (Figure 46) and Benthos' measurement. We cannot compare our *SL* to Benthos' *SL* measurements, however, because we do not know what voltage they applied. However, our maximum measured source levels are the maximum

available, as built. Our measured patterns have a maximum of about 180 dB re 1 μPa-m at 0°. At ±90°, the level drops to about 175 dB re 1 μPa-m. The minimum at 180° is about 160 dB re 1 μPa-m.

In conclusion, the measured beam patterns at 33, 43, and 53 kHz agree with the beam pattern at 40 kHz measured by Teledyne Benthos. However, our measured *SL* is 5 dB higher than that measured by Teledyne Benthos.
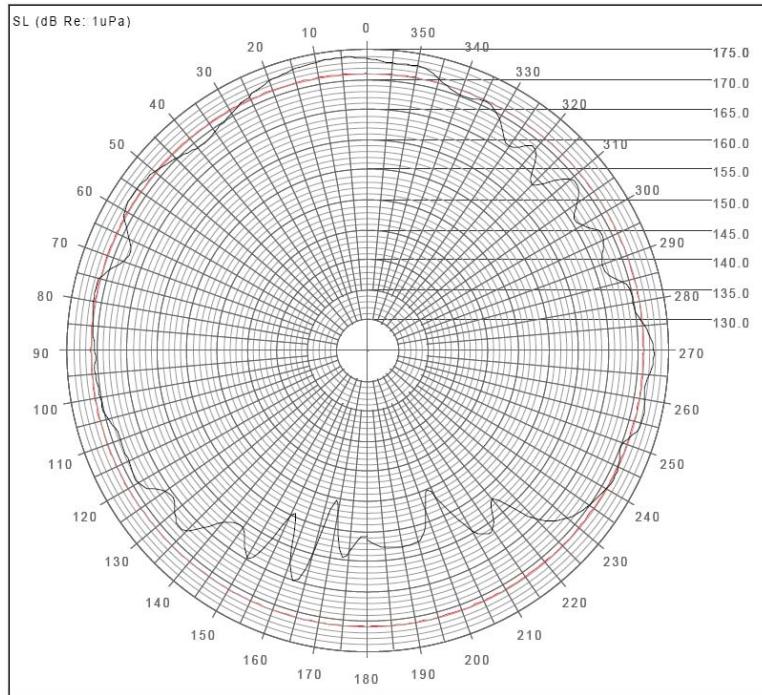
Figure 47.   Benthos-measured source level in the vertical plane at 40 kHz. From [5]

4.   Linearity

Power level should not have an effect on beam pattern. Figure 48 shows that even though maximum power level (08) and -12 dB power level (04) produce about 10 dB difference for the measured frequencies, their beam patterns are very similar.

So the ATM-90X modem displays a good linearity in term of beam pattern for each frequency. At a given frequency, the beam pattern is the same no matter what the power level setting.
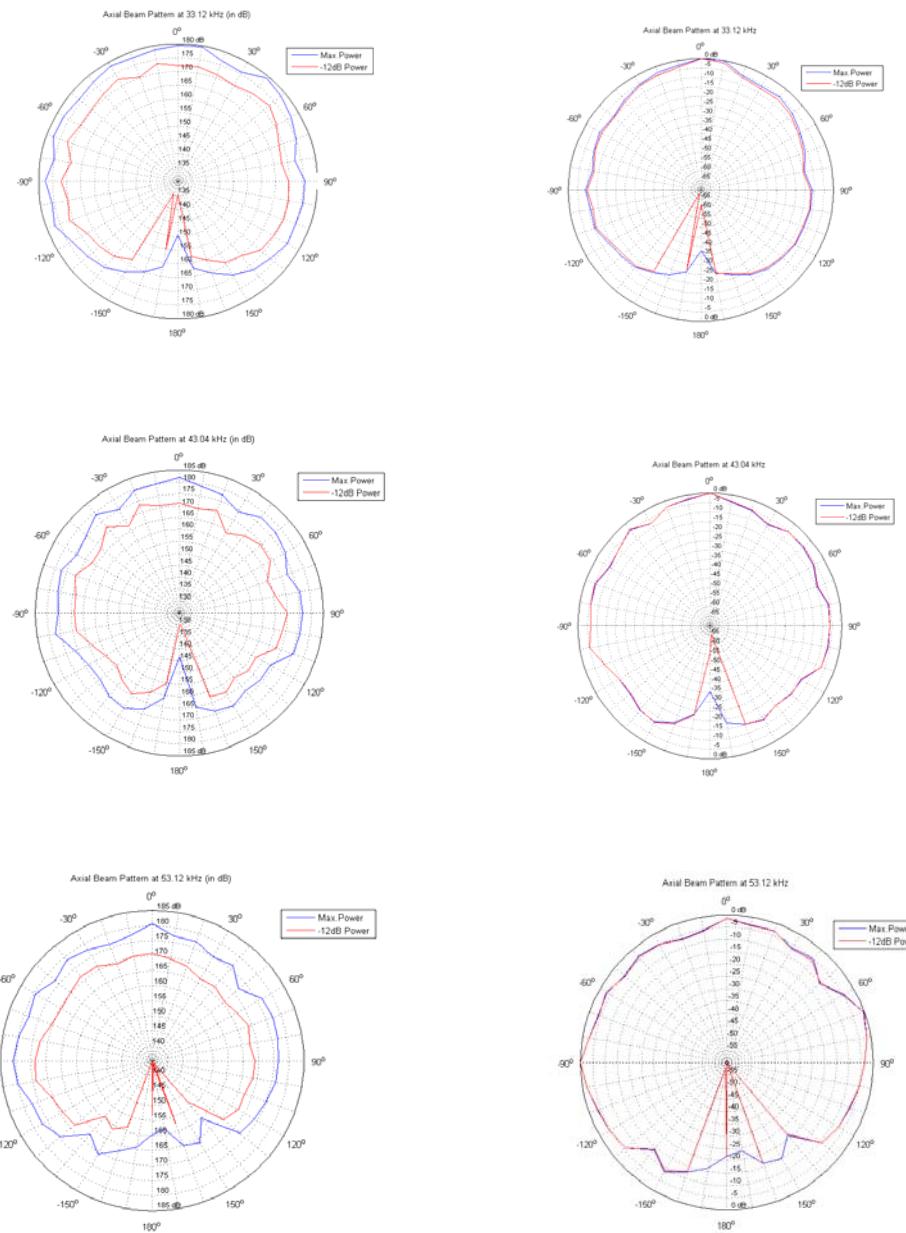
Figure 48. Source level and normalized vertical plane beam patterns measured at frequencies 33, 43, and 53 kHz, with maximum power level (08) and -12 dB power level (04)

THIS PAGE INTENTIONALLY LEFT BLANK

VI.   ANALYSIS OF RESULTS

A.   AVAILABLE SOURCE LEVEL

For the multi-channel 4-ary FSK modulation scheme utilized in Seastar modems, 32 symbols are transmitted simultaneously. The modem hardware limitations require that the maximum signal voltage applied to the internal amplifier input not exceed a certain value, even if all 32 symbols happen to completely constructively interfere. Therefore, the required source level to transmit all 32 symbols is 20*log(32), or about 30 dB greater than would be required for a solitary symbol. This is also verified in the linearity section in Chapter *V* in (5.16).

Conversely, if SL_{max} is the maximum available single-frequency source level, the available source level for transmitting only 1 symbol ($SL_{avail,\ 1sym}$) is given by:

$$SL_{avail,1sym} = SL_{max} - 20\log(I) \ \text{ dB re 1 μPa-m} \tag{6.1}$$

where *I* is number of channels. In our case, *I* is 32, so that:

$$SL_{avail,1sym} = SL_{max} - 30 \ \text{dB} \tag{6.2}$$

The available narrowband source level ($SL_{avail,\ 1sym}$) for the ATM-90X modem is shown in Figure 49. It is essentially the transmit frequency response (source level) reduced by about 35 dB.
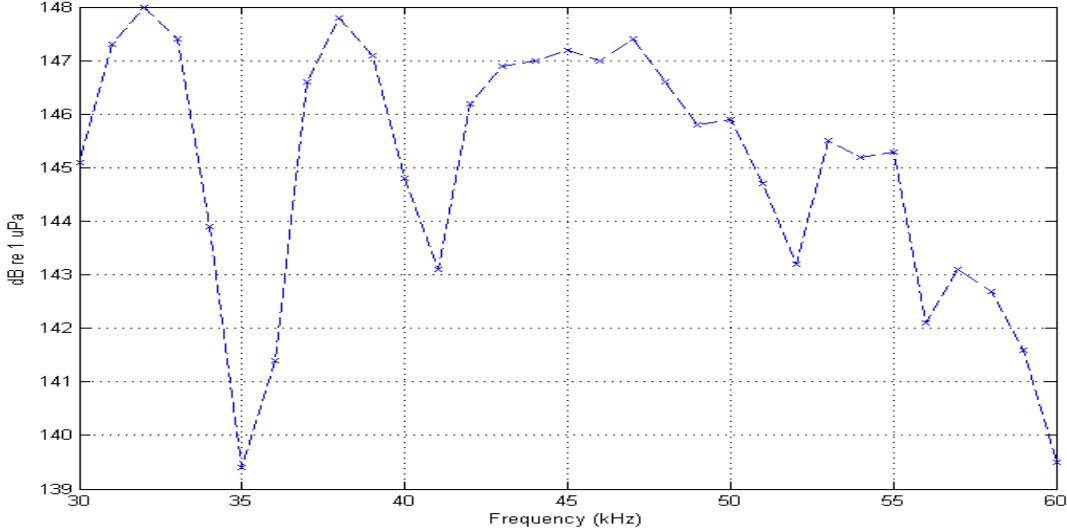
Figure 49.   Available narrowband source level ($SL_{avail, \, 1sym}$)

B.   LINK PERFORMANCE

In this section, the performance of the ATM-90X modem is evaluated.   The available source level ($SL_{avail, \, 1sym}$) is compared against the required narrowband source level for 1 symbol ($SL_{req, \, 1sym}$) in the best (quietest) and worst (noisiest) operating conditions, with spectral bandwidths of 10 kHz and 20 kHz.   This comparison demonstrates the expected operational capability of the ATM-90X modem when using 32 frequencies to simultaneously transmit 32 symbols in the best and worst case scenarios.

1.   General Performance in Best- and Worst-Case Scenarios

a.   Best-Case Scenario

Figure 50 shows the situation where the ATM-90X modem is set to operate with a 10 kHz spectral bandwidth in the best operating condition (quietest).   The $SL_{avail, \, 1sym}$ curve is compared against the curves of $SL_{req, \, 1sym}$ with symbol-transmission probability of success rates of 90%, 95% and 99%.   The $SL_{avail, \, 1sym}$ curve is, at least, approximately about 11.0 dB above the curves of $SL_{req, \, 1sym}$ across the frequency band

between 33 kHz to 55 kHz. Therefore, the ATM-90X modem should be able to successfully support a 500 m communication link with any given 10 kHz bandwidth in the best-case scenario.
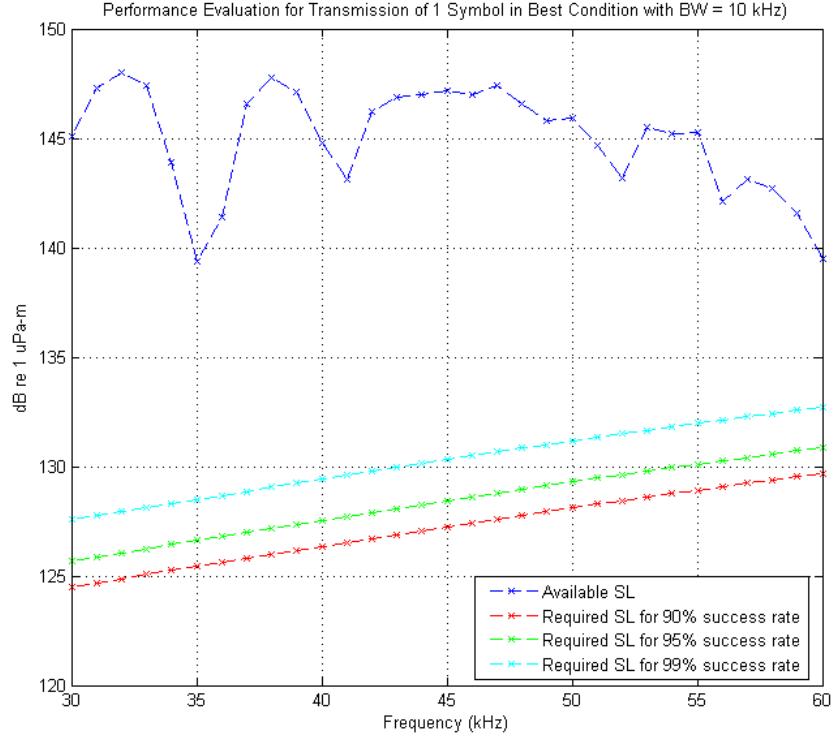
Figure 50. Expected capability of the ATM-90X modem to communicate at the range of 500 m with the uncoded data rate of 4800 bps under the best (quietest) operating condition, using 10 kHz spectral bandwidth

Figure 51 shows the situation where the ATM-90X modem is set to operate with a 20 kHz spectral bandwidth in the best operating condition (quietest). The $SL_{avail,\ 1sym}$ curve is, at least, approximately about 8.0 dB above the curves of $SL_{req,\ 1sym}$ across the frequency band between 33 kHz to 55 kHz. Therefore, the ATM-90X modem should be able to successfully support a communication link with any given 20 kHz bandwidth in the best-case scenario.
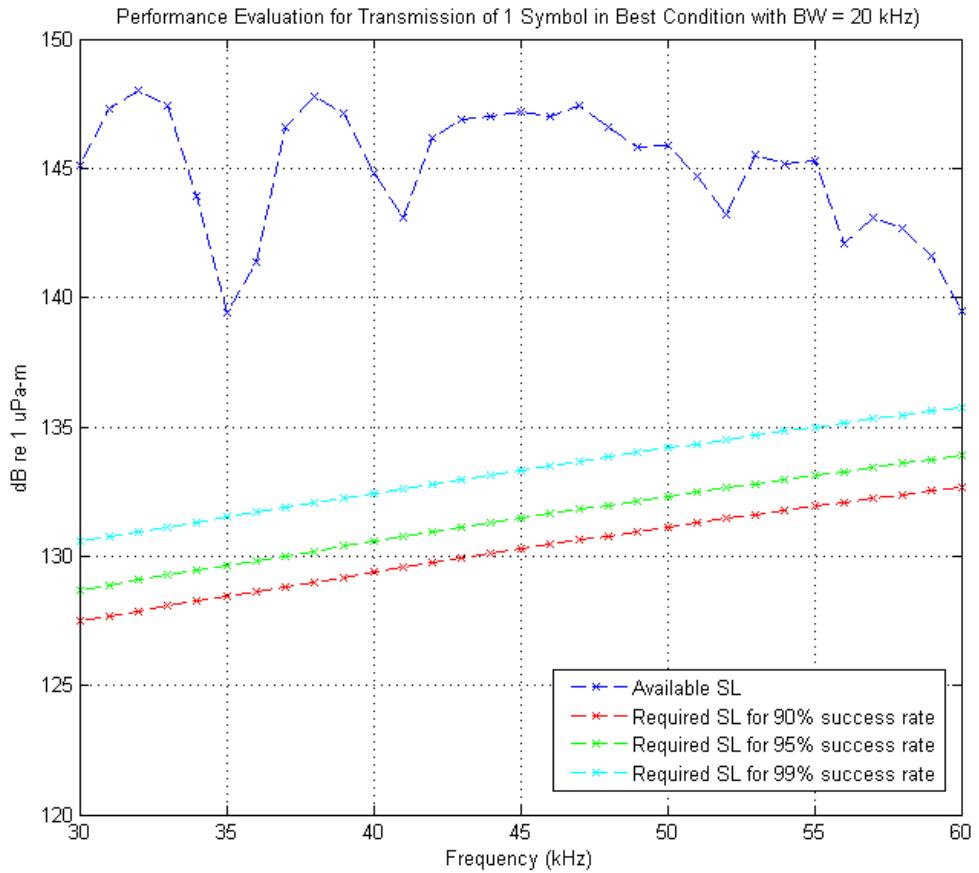
Figure 51.   Expected capability of the ATM-90X modem to communicate at the range of 500 m with the uncoded data rate of 9600 bps under the best (quietest) operating condition, using 20 kHz spectral bandwidth

For the best (quietest) operating condition where there are low wind, shipping and biological noises, the ATM-90X modem should be effective at a range of 500 meters, even without forward error correction coding.

b.   *Worst-Case Scenario*

Figures 52 and 53 show the situations where the ATM-90X modem is set to operate in the worst operating condition (noisiest), with 10 kHz and 20 kHz spectral bandwidths, respectively. Respectively, the $SL_{avail,\ 1sym}$ curves are more than 18.0 dB and 21.0 dB below the curve of $SL_{req,\ 1sym}$, with a symbol-transmission success rate of 90%

across the frequency band between 33 kHz to 55 kHz. Therefore, with the current firmware, the ATM-90X modem cannot support the 500 m communication link in the worst-case scenario.
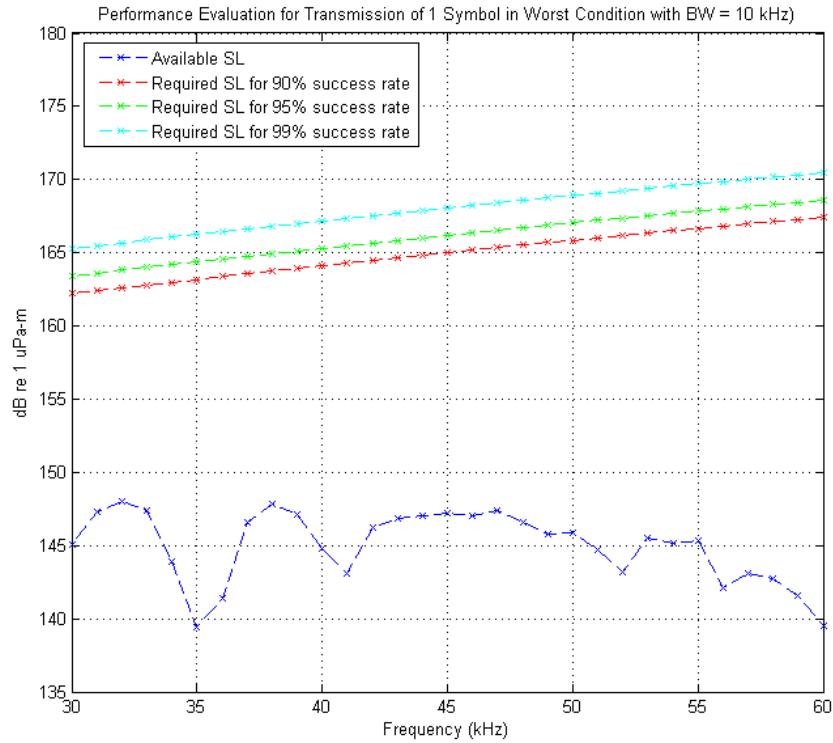
Figure 52.   Expected capability of the ATM-90X modem to communicate at the range of 500 m with the uncoded data rate of 4800 bps under the worst (noisiest) operating condition, using 10 kHz spectral bandwidth
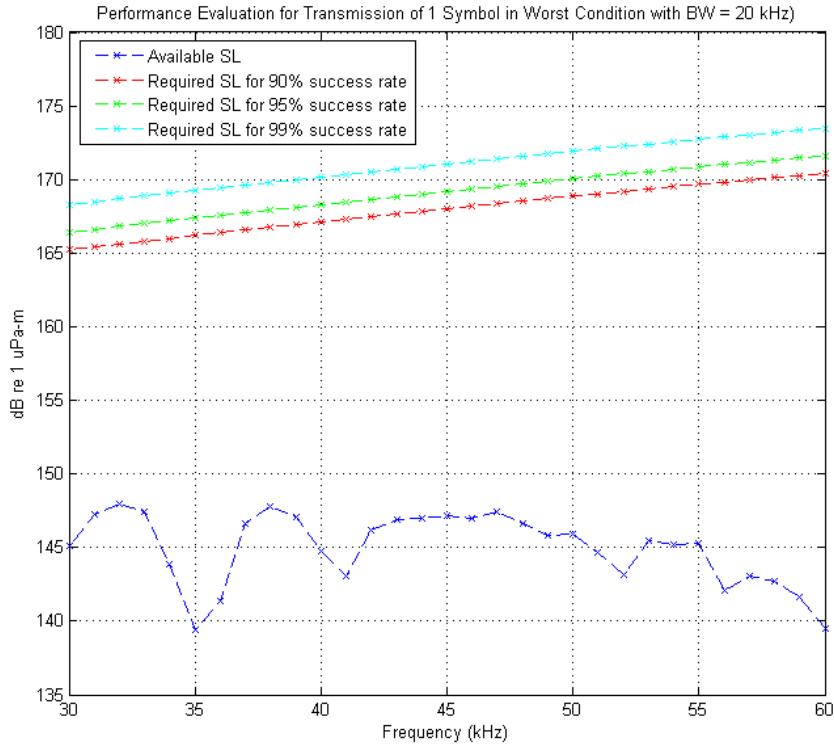
Figure 53.   Expected capability of the ATM-90X modem to communicate at the range of 500 m with the uncoded data rate of 9600 bps under the worst (noisiest) operating condition, using 20 kHz spectral bandwidth

2.   Minimum Link Margin

For our analysis, Link Margin (*LM*) [6] is defined as:

$$LM = SL_{avail,1sym} - SL_{req,1sym} \quad \text{dB} \tag{5.2}$$

LM is the same as signal excess in conventional sonar system analysis. By examining the $SL_{avail, 1sym}$ curve, we expect that the limitation of the communication link would arise from the major null at 35 kHz. The null is about 134.5 dB re 1μPa, approximately 8.0 dB below the maximum level. Therefore, *LM* at 35 kHz would be the minimum *LM* (*LM_{min}*) for our system.

Table 9 assesses *LM_{min}* (*LM* at 35 kHz) for different bit error rates. Positive *LM_{min}* values indicate excess *SNR*. Negative *LM_{min}* values indicate a shortage of *SNR*.

Table 9. LM_{min} comparison between the best- and worse-case scenarios with bandwidths of 10 kHz and 20 kHz for different success rates at 35 kHz

Minimum Link Margin (LM_{min})		99% success rate (dB)	95% success rate (dB)	90% success rate (dB)
10-kHz Bandwidth	**Best Condition (Quietest)**	+11.0	+13.0	+14.0
	Worst Condition (Noisiest)	-27.0	-25.0	-24.0
20-kHz bandwidth	**Best Condition (Quietest)**	+8.0	+10.0	+11.0
	Worst Condition (Noisiest)	-30.0	-28.0	-27.0

From Table 9, operating with 10 kHz bandwidth gives a 3 dB greater *LM* than operating with 20 kHz. For the best operating condition with 10 kHz operating bandwidth and 99% symbol-transmission success rate of detection, the ATM-90X modem has the LM_{min} of 11.0 dB across the entire frequency band of 33–55 kHz. Typically, a *LM* of 6 dB is required for communication link [17]. Therefore, for our case with LM_{min} of 11.0 dB, it should ensure a good performance on the communication link in the best (quietest) operating condition.

If the ATM-90X operates with 20 kHz operating bandwidth in the best operating condition, the LM_{min} is 8.0 dB, which is more than the requirement of 6 dB. Therefore, it should also ensure a good performance on the communication link in the best (quietest) operating condition.

For the worst operating conditions, the $SL_{avail, 1sym}$ must be increased at least 24 dB in order to achieve a communication link with 90% symbol-transmission success rate of detection using 10 kHz bandwidth. Therefore, we conclude that performance on the communication link when operating under the worst (noisiest) condition would be very

poor. In these impaired channel conditions, shorter range links might be achievable with the incorporation of forward error correction codes.

VII. CONCLUSIONS

A. SUMMARY OF FINDINGS

The transmit frequency response, vertical beam pattern and source level of Teledyne Benthos ATM-90X telemetry acoustic modem are as follows. For the transmit frequency response, the maximum response is 183 dB re 1μPa-m at 38 kHz. Transmit frequency response has reasonable flatness (within ± 5 dB from the maximum response) from 37 kHz to 55 kHz. There is one major null at 35 kHz, where the response is about 8.5 dB lower than the maximum response. Vertical beam pattern shows a good hemisphere pattern the top (0°) to broadside (±90°), as observed at the frequencies 33, 43, and 55 kHz. Maximum source level when operating at frequencies between 33 and 55 kHz on broadside is approximately 175 dB re 1μPa-m.

The expected performance when operating under the best (quietest) and worst (noisiest) conditions at the range of 500 m are as follows. In the best operating condition, where wind speed is zero and without significant shipping or biological noise, the ATM-90X modems should be able to support communication links with maximum data rate and symbol-transmission success rate of 99%, using either 10 kHz or 20 kHz bandwidth. In the worst condition, where wind speed is 15 m/s and shipping and biological noises are at the noisiest levels, the ATM-90X modems should not support communication links at 500 m.

Recommendations for practical operations with these prototype modems are as follows. To optimize performance, operational bandwidth should be from 35 kHz to 55 kHz for the 20-kHz bandwidth and from 41 kHz to 51 kHz for the 10-kHz bandwidth. The operational bandwidth of 10 kHz would yield better performance in terms of reliability by a factor of 3 dB in *LM*. However, the maximum data rate reduces to 4800 bps, instead of 9600 bps if using the 20-kHz bandwidth. When there is a presence of high noise level, the operational range can be decreased to 350 m. This range would give a gain of 3 dB in *LM* and, therefore, will increase reliability. Further improvement to the *LM* can be attained through the use if forward error correction and at the expense

of information bit rate. Additional performance gains will result from refinements to the modulation scheme, such as those one recommended by Jenkins [4].

B.   RECOMMENDATION FOR FUTURE WORK

Since the operational performance depends greatly on noise in the operational environment and our estimated operational performance is based on simulated channel and noise, further research on the Teledyne Benthos ATM-90X telemetry acoustic modem should include performance measurements at sea in operating environments where real channel conditions and noise are present.

The experiment should be performed under conditions close to the best (quietest) operating conditions described in this thesis to verify the methodology for making estimation on performance. Furthermore, future in-ocean experiments under varying conditions and in different environments could improve our basis for performance criteria with more empirical data.

Since the vertical beam pattern of the ATM-90X modem is frequency dependent, more experiments with spacing of 20 Hz between each frequency should be performed to verify the beam pattern across the entire operational bandwidth.

Finally, in recognition of the fact that the modems we evaluated for this thesis are prototype devices, we recommend improvements to the next iteration on this modem design. In particular, we urge careful design of a matching network to produce a flat 20-kHz operating band.

LIST OF REFERENCES

[1]   M. C. Goh, "Event-driven simulation and analysis of an underwater acoustic local area network," M.S. thesis, Naval Postgraduate School, Monterey, CA, 2010.

[2]   J. A. Rice and D. Green, "Advances in acoustic communications and undersea networks," in *Proc. MAST 2008 Conf.*, Cadiz, Spain, 2008.

[3]   B. Kerstens, "A study of the Seastar Underwater Acoustic Local Area Network concept," M.S. thesis, Naval Postgraduate School, Monterey, CA, 2007.

[4]   W. Jenkins, "Time/frequency relationships for an FFT-based acoustic modem," M.S. thesis, Naval Postgraduate School, Monterey, CA, 2010.

[5]   K. Scussel and K. Amundsen. *Seastar Short-Range Modems, Transducer Performance Report*. North Falmouth, MA:Teledyne Benthos (2009).

[6]   J. T. Hansen, "Link budget analysis for undersea acoustic signaling," M.S. thesis, Naval Postgraduate School, Monterey, CA, 2002.

[7]   L. E. Kinsler, A. R. Frey, A. B. Coppens and J. V. Sanders, *Fundamentals of Acoustics*, 4th ed. New York: John Wiley & Sons, 2000.

[8]   C. D. McGillem and G.R. Cooper, *Continuous and Discrete Signal and System Analysis*, 3rd ed. Chicago, IL: Saunders College Publishing, 1991.

[9]   A. L. Maggi and A. J. Duncan. (Accessed Feb. 2010). AcTUP v2.2*l*α Acoustic Toolbox User-interface & Post-processor: Installation & User Guide. Curtin University of Technology, Centre for Marine Science & Technology. Perth, Australia. [Online]. Available: http://cmst.curtin.edu.au/local/docs/products/actup_v2_2l_installation_user_guide.pdf

[10]   J. C. Torres, "Modeling of high-frequency acoustic propagation in shallow water," M.S. thesis, Naval Postgraduate School, Monterey, CA, 2007.

[11]   S. R. Thompson, "Sound Propagation Considerations for a Deep Ocean Acoustic Network," M.S. thesis, Naval Postgraduate School, Monterey, CA, 2009.

[12]   R. F. W. Coates, *Underwater Acoustic Systems*. New York: Halsted Press, 1989.

[13]   R. J. Urick, *Principles of Underwater Sound*, 3rd ed. Los Altos Hills, CA: Peninsula Publishing, 1983.

[14]   J. G. Proakis and M. Salehi, *Communication Systems Engineering*, 2nd ed. Upper Saddle River, NJ: Pearson Prentice Hall, 2002.

[15]   M. Stojanovic, "Underwater acoustic communication," in *Wiley Encyclopedia of Electrical and Electronics Engineering*, John G. Webster, Ed. New York: John Wiley & Sons, 1999.

[16]   I. F. Akyildiz, D. Pompili and T. Melodia, "Underwater acoustic sensor networks: Research challenges," Ad Hoc Networks (Elsevier), vol. 3, no. 3, 257– 279, May. 2005.

[17]   J. G. Proakis, *Digital Communications*, 4th ed. New York: McGraw-Hill, 2001.

[18]   D. Green. *Design Specifications, Seaweb Telesonar Header Packet*. North Falmouth, MA: Teledyne Benthos, 2009.

[19]   Teledyne Benthos Staff, *Acoustic Telemetry Modem User's Manual*, Teledyne Benthos, P/N 003452, rev. F, Mar. 2006.

[20]   Teledyne Benthos Staff, *4th Generation Modem FFS Play Command HOWTO*. Teledyne Benthos. North Falmouth, MA. [Print].

[21]   G. S. Sineiro, "Underwater multimode directional transducer evaluation," M.S. thesis, Naval Postgraduate School, Monterey, CA, 2003.

[22]   C. H. Sherman and J. L. Butler, *Transducers and Arrays for Underwater Sound.* New York: Springer Science+Business Media, LLC, 2007.

INITIAL DISTRIBUTION LIST

1.   Defense Technical Information Center
        Ft. Belvoir, Virginia

2.   Dudley Knox Library
        Naval Postgraduate School
        Monterey, California

3.   Steve Baker
        Department of Physics
        Naval Postgraduate School
        Monterey, California

4.   Joseph Rice
        Department of Physics
        Naval Postgraduate School
        Monterey, California

5.   Daphne Kapolka
        Department of Physics
        Naval Postgraduate School
        Monetery, California

6.   RADM (Ret.) Jerry Ellis, USN
        Naval Postgraduate School
        Monetery, California

7.   RADM (Ret.) Rick Williams, USN
        Naval Postgraduate School
        Monetery, California

8.   Dale Green
        Teledyne-Benthos
        Falmouth, Massachusetts

9.   Ken Scussel
        Teledyne-Benthos
        Falmouth, Massachusetts

10.   Chris Fletcher
        SPAWAR Systems Command Pacific
        San Diego, California

11. Paul Gendron
    SPAWAR Systems Command Pacific
    San Diego, California

12. Mihailo Tomic
    SPAWAR Systems Command Pacific
    San Diego, California

13. Bob Creber
    SPAWAR Systems Command Pacific
    San Diego, California

14. Mark Gillcrist
    SPAWAR Systems Command Pacific
    San Diego, California

15. Leroy Sverduk
    Office of Naval Research
    Arlington, Virginia

16. LCDR Bjørn Kerstens
    Royal Netherlands Navy
    Netherlands

17. MAJ Meng Chong Goh
    Republic of Singapore Navy
    Singapore

18. LTJG Pongsakorn Sommai
    Royal Thai Navy
    Thailand

19. ENS William F. Jenkins II, USN
    Naval Postgraduate School
    Monterey, California